# Modelling river-sea continuum: the case of the Danube Delta

Christian Ferrarin[1], Debora Bellafiore[1], Alejandro Paladio Hernandez[1], Irina Dinu[2], and Adrian Stanica[2]

[1]CNR - National Research Council of Italy, ISMAR - Marine Sciences Institute, Venice, Italy
[2]National Institute of Marine Geology and Geoecology - GeoEcoMar, Bucharest, Romania

**Correspondence:** Christian Ferrarin (christian.ferrarin@cnr.it)

**Abstract.** Understanding water transport and circulation in coastal seas and transitional environments is ~~among the key topics~~ a key focus of oceanographic and climate research, ~~as well as~~ particularly in recognizing the role of the land-sea interface. The Danube Delta ~~represents~~ serves as a natural laboratory for river-sea hydrodynamic modelling due to its complex morphology~~and being subjected to several~~ , composed of multiple river branches, channels, and lagoons. Moreover, this coastal environment is subjected to various natural and anthropogenic stressors, and numerical modelling can provide a scientific basis for assessing the impact of human activities. In this work, ~~we present the results of~~ the SHYFEM finite element hydrodynamic model ~~application to the whole~~ was applied to the entire river-sea continuum of the Danube Delta region to describe the transport and mixing processes within and between the interconnected water bodies forming the delta. The model was run for ~~several years to characterize:~~ the period 2015-2019 and enabled the characterization of: (1) ~~the~~ water discharge distribution among the river branches~~, ~~; (2) ~~the~~ general hydrodynamic characteristics of the coastal region of freshwater influence~~, ~~; (3) ~~the~~ transport time scale of the Razelm Sinoie Lagoon System~~, and 4) the processes driving the river-lagoon-sea interconnections. The unique numerical description of the transport and mixing in the different water bodies of the Delta (river branches, channels, lagoons and coastal sea) may be used to provide the scientific basis to assess the impact of human activities and to design efficient management choices. Indeed, we used the modelling framework~~ . Finally, the Danube Delta modelling tool was used to evaluate the ~~effect of~~ potential effects of hydrological reconnection (restoration) measures in the Razelm Sinoie Lagoon System ~~designed to improve hydrological connectivity~~ aimed at improving connectivity and water renewal.

## 1 Introduction

Coastal environments at the river-sea interface, like estuaries and deltas, are critical components of coastal ecosystems due to their importance in supporting biodiversity and providing ecosystem services such as nutrient cycling, carbon sequestration, and habitat for marine life (Newton et al., 2023, and references therein). However, these regions are highly sensitive to both natural events (e.g., storms, sea-level rise, droughts) and anthropogenic pressures (e.g., damming, land reclamation, pollution). As such, modelling these environments is essential for understanding their dynamics, predicting their responses to environmental change, and guiding sustainable management practices.

Modelling ~~these coastal transitional water systems~~ estuaries and deltas is challenging due to their complex morphology made of different components such as river network, coastal lakes, lagoons, creeks, marshes. These different water compartments are generally interconnected and thus influencing each other. In this context, unstructured ocean models, like SCHISM (Zhang

et al., 2016), SHYFEM (Umgiesser et al., 2022), FESOM-C (Androsov et al., 2019), Delft3D (D-Flow, 2023), TELEMAC (Telemac-Mascaret, 2022), ADCIRC ~~(?)~~(Zhang and Yu, 2025), FVCOM (Chen et al., 2003), SLIM (Vallaeys et al., 2018) have proven to be powerful tools for simulating complex hydrodynamics in shallow estuarine and deltaic environments. These models help assess the effects of climate change (Ferrarin et al., 2014; Pein et al., 2023), human interventions (Ferrarin et al., 2013; Thanh et al., 2020), and natural variability on the structure and functioning of coastal systems (Maicu et al., 2018; Zhu et al., 2020; Feizabadi et al., 2024). Models used in estuarine and delta research typically integrate hydrodynamics, sediment transport, water quality, and ecological processes. However, the higher the complexity of the processes to be investigated, the higher is the amount of data needed for the model implementation and testing.

~~In thisstudy~~This paper investigates the hydrodynamic processes, water exchange, and connectivity among the various interconnected water compartments - river branches, channels, lagoons, and the coastal sea - that together form the Danube Delta river–sea continuum. To achieve this, we implemented the SHYFEM ~~(System of HydrodYnamic Finite Element Modules; Umgiesser et al., 2022) model to~~ model (System of HydrodYnamic Finite Element Modules; Umgiesser et al., 2022) across the entire Danube Delta~~region consisting of about~~ , encompassing approximately 500 km of the river network, the Razelm~~– Sinoie lagoon system –~~Sinoie Lagoon System, and part of the prodelta coastal sea ~~. This manuscript focuses on the investigation of hydrodynamics in the river-lagoon-sea system and the hydrological connectivity among the different water bodies (river branches, channels, lagoons, coastal sea). In particular, we apply the model to quantify water discharge distribution among the~~ (Fig. 1). The model outputs are used to quantify the distribution of water discharge among river branches, ~~the dynamics of the coastal sea in front of the multi-mouth delta, the~~ assess the influence of multiple river plumes on coastal dynamics, and analyze the water exchange and renewal capacity of the Razelm–Sinoie Lagoon System~~and the processes regulating the exchange among the different water environments forming the Danube Delta~~. Moreover, ~~a few what-ifscenarios were simulated to explore~~ the numerical tool is used to assess the potential impacts of different hypothetical lagoon-sea reconnection solutions (*what-if* scenarios) on the processes regulating the exchanges between the river, lagoon, and sea.

### 1.1 The Danube Delta

The Danube Delta is the final part of the Danube River's journey of almost ~~2900~~ 2,900 km, crossing 10 countries and draining a hydrographic basin of over 800,000 km$^2$ from 19 states towards its connection with the Black Sea (e.g., Panin, 1998). The Danube Delta plain begins at the first bifurcation of the Danube, called Ceatal Izmail (Fig. 1). Here, the Danube River divides into two distributaries: the northern one, Chilia, and the southern one, Tulcea. The Chilia distributary creates a natural border between Romania and Ukraine. The Tulcea distributary divides again at Ceatal, 17 km farther downstream, into two other branches, Sulina and Sf. Gheorghe. The fluvial delta plain covers ~~4000~~ 4,000 km$^2$ and the marine one covers ~~1800~~ 1,800 km$^2$. The Romanian ~~part~~ section of the Danube Delta, including ~~here the attached Razelm Sinoie~~ the Razelm-Sinoie Lagoon System, was ~~declared in 1991~~ designated a Biosphere Reserve ~~(UNESCO~~in 1991 under UNESCO's "Man and the Biosphere" Programme ~~) and has been ever since~~ and has remained a Nature Reserve ever since.

The Razelm Sinoie Lagoon System (hereinafter RSLS) extends ~~on about 1000~~ for about 1,000 km$^2$ and is located in the southern part of the Danube Delta Biosphere Reserve. RSLS is a semiclosed shallow water body (the average depth is 1.8

m)receiving Danube freshwater from the Dunavăţ and Dranov canals and exchanging waters with the Black Sea via the Edighiol and Periboina inlets. The lagoon system is suffering from poor water renewal and stagnation (Dinu et al., 2015) and has been significantly affected by human interventions since the end of the 19th ~~Century (Panin, 1996, 1998, 1999; Giosan et al., 2006; Vespremeanu~~ century (Panin, 1996, 1998, 1999; Giosan et al., 2006; Vespremeanu-Stroe et al., 2013; Constantinescu et al., 2023). Dredging works to connect the Razelm lagoon to the Sf. Gheorghe arm of the Danube via the Dunavăţ and Dranov canals ~~, ended up~~ were finalized at the beginning of the 20th century. ~~Thus, more freshwater discharged to~~ As a result, more fresh water is discharged into the lagoon system. During the 1950s, management plans were made to decrease the salinity in the lagoon system, with the purpose to increase the freshwater fish culture productivity. Between 1960 and 1990, the lagoon has been used mainly for irrigations and, secondly, for fish breeding. In 1973, the Portiţ~~Inlet (near the reconnection option named A Fig. 1)~~ a Inlet of the Razelm Lagoon was completely closed by a system of breakwaters and groins. ~~Consequently, the coastal erosion increased in intensity south of the former inlet, due to the hard coastal defence structure (??). After~~ Following the closure of the Portiţ~~inlet in the Razelm lagoon has been transformed into freshwater lakes, due to the permanent connection with the Danube River~~ a inlet, the Razelm Lagoon was transformed into a a freshwater lake, receiving Danube water via Dranov and Dunavăţ Canals. The inlet of Gura Buhazului ~~(near the reconnection option named C Fig. 1)~~ in the southern part of the Sinoie Lagoon was clogged more than 3 decades ago (late 1980s - early 1990s). The permanent circulation between the Sinoie Lagoon and the Black Sea has been restored by the beginning of the years 2000, being controlled by the Periboina and Edighiol inlets. The Periboina inlet has become clogged around 2017, with an intermittent connection with the sea during spring and autumn months up to the year 2021. ~~Anyway, a major hydrotechnical project is underway as~~ As part of the ~~Masterplan for the Protection against Erosion~~ master plan for the protection of the Romanian Littoral ~~- project that would secure~~ against erosion, a major hydraulic engineering project is currently implemented, to ensure a permanent water exchange ~~for~~ through the Periboina Inlet.

The Danube River ~~in its lower part~~ before the delta has an average water discharge of ~~6500~~ 6,500 $m^3\ s^{-1}$ ~~and~~ , with values ranging from ~~2000 to 16000~~ 1,300 to 16,000 $m^3\ s^{-1}$ (Pekárová et al., 2021). The two major wind regimes characterizing the study area are from north-east, being the most intense, and south-south-west, that can drive alongshore water and sediment transport (Dan et al., 2009).

## 2 Methods

### 2.1 The modelling system

In this study, we used the System of HydrodYnamic Finite Element Modules (SHYFEM, Umgiesser et al., 2022) model to simulate the three-dimensional (3D) hydrodynamics in the river-sea continuum of the whole Danube Delta region. SHYFEM is an open-source unstructured ocean model for simulating hydrodynamics and transport processes at very high resolution. The model solves the primitive equations written in z-coordinate system and using a finite element numerical method and semi-implicit time stepping. The model has been already applied to simulate the hydrodynamics in the Mediterranean Sea (Ferrarin et al., 2018), in the Adriatic Sea (Bellafiore et al., 2018; Ferrarin et al., 2019), in the Black Sea ~~(Bajo et al., 2014; Bellafiore et al., in review)~~ (Bajo et al., 2014) and in several coastal systems (Ferrarin et al., 2021; Umgiesser et al., 2022).

~~SHYFEM is here used to reproduce the 3D hydrodynamics of the Danube Delta under the influence of river discharge, heat and momentum fluxes at the water surface, salinity and sea temperature gradients and open sea forcing (sea level oscillations and currents). Moreover, the concurrence of intense atmospheric forcing, direct morphological interventions within the delta territory and freshwater inflows lead the Danube Delta to be characterized by a wide range of different transport phenomena. Therefore, to investigate water mixing and renewal, the numerical model has been used to estimate the transport time scale, which is a fundamental parameter for understanding chemical and ecological dynamics in lagoon environments (Cucco et al., 2009). In this study, the water renewal time (hereinafter WRT) was computed by simulating the transport and diffusion of a Eulerian conservative tracer released uniformly throughout the entire lagoon system with a concentration corresponding to 1, while a concentration of zero was imposed on the seaward and freshwater boundaries. The local WRT is considered as the time required in each water parcel for the tracer concentration to fall to 0. The reader may refer to Cucco et al. (2009) and Umgiesser et al. (2022) for a more comprehensive description of the WRT computation.~~

The SHYFEM model was applied to a domain that comprises the river network of the Danube Delta from Isaccea (100 km upstream from the river mouths, in the vicinity of the delta apex at Ceatal Izmail) to the sea (from north to south the Chilia, Sulina and Sf. Gheorghe branches), the Razelm Sinoie Lagoon System, the nearby prodelta and shelf area (290x100 km) and the narrow canals and inlets connecting the different water compartments (Dunavăţ, Dranov, Canal 2, Canal 5, Edighiol and Periboina) (Fig. 1). The application of a triangular unstructured grid in the hydrodynamic model has the advantage of describing accurately complicated bathymetry and irregular boundaries in the river and shallow water areas. It can also solve the combined offshore-coastal interactions and small-scale river-sea dynamics in the same discrete domain by subdividing the basin into triangles varying in form and size. The unstructured mesh is generated using the mesh-generation software GMSH (Geuzaine and Remacle, 2009). The numerical domain is composed of about ~~48.000~~ 48,000 triangular elements having horizontal resolution varying from about 4 km in the open sea to a few metres in the river branches and the connecting channels. Vertically, the model runs in ~~the~~ z layer configuration, with 68 layers of increasing thickness, from 1 m in the topmost layers, to 50 m in the deepest ones (below 500 m).

The model bathymetry is obtained by a bilinear interpolation on the numerical grid of the following available datasets (all referred to the Marea Neagra Sulina vertical datum):

- the 2022 European Marine Observation and Data Network dataset (EMODnet Bathymetry Consortium, 2022) for the shelf sea on a regular grid of 1/16*1/16 arc minutes, ca. 115 metre grid;
- the 2024 dataset for the Razelm Sinoie Lagoon System ~~;~~ acquired on (mostly West-East-oriented) transects spaced 450 m apart on average and covering the whole system. The distance between two points within each transect is $\sim$1 m.
- three separate ~~datasets~~ multibeam datasets (provided at a $\sim$1 m resolution) for the main river branches: the 2023 dataset for Chilia; the 2019 dataset for Sulina; the 2016-2017 dataset for Sf. Gheorghe. Available sparse data was used for some secondary branches and small channels.

The maximum allowable time step in the simulation was set to 60 s, and the model adopts automatic sub-stepping over time to enforce numerical stability with respect to advection and diffusion. The wind drag coefficient was set to 2.5 $10^{-3}$.

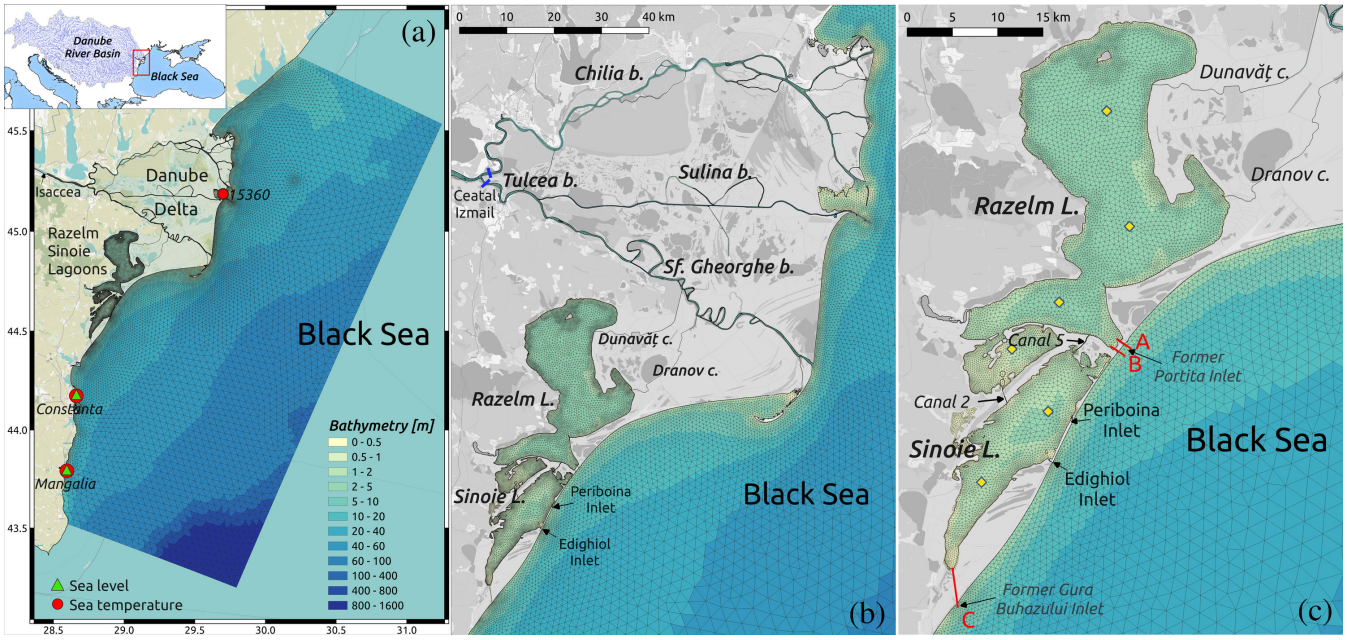


**Figure 1.** (a) Unstructured numerical grid and bathymetry of the hydrodynamic model of the Danube Delta and Black Sea shelf with the red dots and the green triangles marking the sea temperature and sea level monitoring stations, respectively; (b) zoom of the grid over the Danube Delta with the blue bars near Ceatal Izmail indicating the river discharge monitoring stations; (c) zoom of the grid over the Razelm Sinoie Lagoon Systems with the red bars illustrating the considered reconnection solutions and the yellow diamonds marking the satellite SST control points. Background: ©OpenStreetMap contributors 2024; distributed under the Open Data Commons Open Database License (ODbL) v1.0.

Bottom friction is computed following the Strickler formulation (Umgiesser et al., 2004) with the friction parameter considered homogeneous over the whole domain and set equal to 32 $m^{1/3}$ $s^{-1}$. Vertical diffusivities are calculated by the $k-e$ turbulence closure model. Model outputs are saved at a daily frequency. This choice was made to limit the volume of model outputs and is justified by the fact that the boundary conditions for the open sea and the river have a daily frequency.

To investigate how the difference forcing and processes influence the water mixing and renewal in the semiclosed Razelm Sinoie Lagoon System, the numerical model has been used to estimate two transport time scales: the water flushing time (WFT) and the water renewal time (WRT) (Umgiesser et al., 2014). The basin-wide WFT is defined as the theoretical time necessary to replace the complete volume of the water body with new water and assuming a hypothetical fully mixed basin and is computed diving the basin volume by the volumetric water flux flowing out of the system. WRT is computed by simulating the transport and diffusion of a Eulerian conservative tracer released uniformly throughout the entire lagoon system with a concentration corresponding to 1, while a concentration of zero was imposed on the seaward and freshwater boundaries. The local WRT is considered as the time required for each cell of the RSLS to replace the mass of the conservative tracer, originally released, with new water. The ratio between the basin wide WFT and WRT can be interpreted as an index of the mixing behaviour of

the basin. The reader may refer to Cucco et al. (2009) and Umgiesser et al. (2022) for a more comprehensive description of the transport time scales.

### 2.2 Numerical experiments

SHYFEM is here used to reproduce the 3D hydrodynamics of the Danube Delta under the influence of river discharge, heat and momentum fluxes at the water surface, salinity and sea temperature gradients and open sea forcing (sea level oscillations and currents). Moreover, the concurrence of intense atmospheric forcing, direct morphological interventions within the delta territory and freshwater inflows lead the Danube Delta to be characterized by a wide range of different transport phenomena.

To reproduce the past sea conditions over the period ~~2015-2020~~2014/01/01 - 2019/12/31, the simulations were forced by 3-hourly wind, mean sea level pressure, air temperature, relative humidity, incident solar radiation, total precipitation and cloud cover fields from Copernicus European Regional ReAnalysis (CERRA; Schimanke et al., 2021) made available via the Copernicus Climate Change Service (https://doi.org/10.24381/cds.622a565a). CERRA has a horizontal resolution of 5.5 km and is forced by the global ERA5 reanalysis (Hersbach et al., 2020). The SHYFEM hydrodynamic model was forced at the lateral boundary of the Black Sea with ~~the~~ daily sea level, current velocity, sea temperature and salinity fields from the Black Sea Physics Reanalysis made available via the E.U. Copernicus Marine Service Information (Lima et al., 2020, https://doi.org/10.25423/CMCC/BLKSEA_MULTIYEAR_PHY_007_004, accessed on 14-Jun-2024). Daily observed water river discharges at Isaccea were provided by the National Institute of Hydrology and Water Management of Romania and imposed as a boundary condition for the Danube River. Water temperature at the Danube River boundary was taken from the daily results of the ~~wflow~~ *wflow* catchment model implemented over the Danube River basin ~~(Bellafiore et al., in review)~~ (van Gils et al., 2025).

~~The maximum allowable time step in the simulation was set to 60 s, and the model adopts automatic sub-stepping over time to enforce numerical stability with respect to advection and diffusion. The wind drag coefficient was set to 2.5 $10^{-3}$. Bottom friction is computed following the Strickler formulation (Umgiesser et al., 2004) with the friction parameter considered homogeneous over the whole domain and set equal to 32 $m^{1/3}$ $s^{-1}$. Vertical diffusivities are calculated by the $k-\epsilon$ turbulence closure model.~~

~~Being aware that the RSLS is suffering from poor water renewal and stagnation (Dinu et al., 2015), the model was used~~ In the past, the lagoons were connected to the sea via several inlets, while nowadays only the Periboina and Edighiol connections remain open. Additional numerical experiments were conducted to investigate the potential effects on ~~WRT and salinization~~ the lagoons' water renewal and salinisation of different reconnection solutions designed in collaboration with local stakeholders to ~~improve~~ enhance the river-lagoon-sea exchange. The dredging of a new inlet is under consideration by local communities and authorities, as part of the activities developed under the framework of the Horizon Europe Project DANUBE4all (https://www.danube4allproject.eu/). The three *what-if* scenarios considered in this study consisted of opening ~~a~~ one 1.5 m depth and 70 m wide channel to connect the either the Razelm Lagoon (~~red bars marked~~ solutions A and B in Fig. 1c) ~~and~~ or the Sinoie Lagoon (~~red bar marked~~ solution C in Fig. 1c) with the Black Sea. These reconnection solutions are located in the vicinity of previous inlets, now either closed by humans (Portiţa~~; solutions A and B) or now~~ ) or clogged (Gura Buhazului inlet, active

till the beginning of the 1990s~~; solution C~~). The period, parametrization, forcing and boundary conditions considered in these *what-if* numerical experiments are the same as those adopted in the reference run (hereinafter called REF).

In all simulations, the entire year 2014 is considered as the model's spin-up time, and the results are analyzed over the period 2015-2019.

### 2.3 ~~The~~ Model validation~~datasetThe monitored parameters~~

The application of the SHYFEM model to the Danube Delta was validated by comparing various parameters. The validation aims at assessing the skill of SHYFEM model in reproducing the hydrodynamics in the different water compartment of the delta. The available datasets used in the validation procedures are grouped into the following ~~three~~ four categories:

- In-situ river discharge: daily values are provided by the National Institute of Hydrology and Water Management of Romania for two river sections near Ceatal Izmail where the Danube River splits into the Chilia and Tulcea branches (blue bars in Fig. 1b). The Tulcea branch downstream splits into the Sulina and Sf. Gheorghe arms, but no observations were available for these branches.

- In-situ sea level: hourly values were retrieved from the in-situ ocean thematic centre of the Copernicus Marine Service (https://marineinsitu.eu/dashboard/) for stations Constanta and Mangalia (green triangles in Fig. 1a).

- In-situ sea temperature: daily values were retrieved from the in-situ ocean thematic centre of the Copernicus Marine Service (https://marineinsitu.eu/dashboard/) for BS_TS_MO stations 15360, 15480 (Constanta) and 15499 (Mangalia) (red dots in Fig. 1a).

- Satellite Sea Surface Temperature (SST): Level 2 data derived from the Landsat-8 Thermal Infrared Sensor (TIRS) extracted over six locations within the Razelm Sinoie Lagoon to cover the spatial variability in the lagoons (yellow diamonds in Fig. 1c). The SST data are generated through the application of an atmospheric correction algorithm to the Top-Of-Atmosphere thermal radiance values from the TIRS bands (B10 and B11). This algorithm accounts for atmospheric effects such as water vapor and aerosol interference and applies a split-window technique to estimate surface temperatures with high accuracy (Barsi et al., 2003). The data, provided by the United States Geological Survey (USGS), were accessed via the Google Earth Engine platform using the LANDSAT/LC08/C02/T1_L2 dataset. To ensure data quality and reliability, scenes with cloud cover below 1% were selected, effectively minimizing the impact of atmospheric interference. For each location, SST values were extracted at midnight using a 1x1 pixel window, corresponding to the nearest pixel to the specified coordinates. A total of ~~37~~ 31 time frames providing 135 valid SST observations were selected in the period from 2015 to ~~2020.~~ 2019.

**Table 1.** Statistical analysis of simulated river discharge, sea level, sea temperature and sea surface temperature.

| Variable | Station | N data | RMSE | BIAS | CC | SLOPE |
|---|---|---|---|---|---|---|
| River discharge ($m^3$ $s^{-1}$) | Chilia | 120 | 158 | -46 | 1.00 | 0.90 |
| | Tulcea | 120 | 158 | 43 | 1.00 | 1.10 |
| Sea level (cm) | Constanta | 624 | 6.5 | - | 0.66 | 0.70 |
| | Mangalia | 722 | 7.8 | - | 0.55 | 0.62 |
| Sea Temperature (°C) | 15360 | 972 | 1.7 | 0.2 | 0.98 | 1.08 |
| | Constanta | 966 | 1.6 | -0.4 | 0.97 | 0.98 |
| | Mangalia | 908 | 1.5 | -0.2 | 0.97 | 0.96 |
| SST (°C) | Razelm Sinoie | 135 | 1.0 | 0.3 | 0.97 | 0.99 |

## 3 ~~Results~~

### 2.1 ~~Model validation~~

In this work, we consider the root mean square error (RMSE), the difference between the mean of simulation results and observations (BIAS), the Pearson ~~cross-correlation~~ correlation coefficient between model results and observations (CC) and the slope of the linear regression best-fit line (SLOPE) as the metrics for measuring the accuracy of the numerical results of the reference simulation~~in representing the~~ . The results of the statistical analysis of river discharge, sea level and sea temperature ~~variability~~are reported in Table 1.

As shown in Fig. 2a, the Danube River discharge at Isaccea (the upstream river boundary in the model domain) in the period 2015-2019 varies from ~~2000 to 14000~~ 2,000 to 14,000 $m^3$ $s^{-1}$ with an average value of about ~~6000~~ 6,000 $m^3$ $s^{-1}$. Figures 2b and 2c represent the scatter plots of observed and simulated river discharge through the Chilia and Tulcea river branches at Ceatal Izmail. The model well represents the total water discharge distribution in the Chilia and Tulcea branches, with a RMSE of 158 $m^3$ $s^{-1}$ and CC of 1.00 in both distributaries (Table 1). It is worth noting that the model tends to underestimate (overestimate) the peak discharge values in the Chilia (Tulcea) arm, as revealed also by a slope of the linear regression best-fit line of ~~0.89 (1.11). Since in flood events there is a possible enlargement of the river section, including floodplains, probably a lack of information on the altimetric quotes around the river can justify this small inconsistency. The model has a RMSE of about 160 $m^3$ $s^{-1}$ in both distributaries~~0.90 (1.10). The underestimation at Chilia coincides with situations of overestimation at Tulcea. The inconsistency during flood events is likely attributable to the model's inability to correctly reproduce the river overflow into the surrounding floodplains.

We report in Figure 3, the time series of the modelled daily sea levels compared with the observations for 2017 at the coastal stations Constanta and Mangalia located along the Romanian coast (green triangles in Fig. 1a). The model can reproduce the long-term sea level variability as well as the major fluctuations associated with intense meteorological events (storm surges) ~~in the range of 1-10~~ with typical time scales of 1 to 10 days. The model is slightly underestimating sea levels in some periods

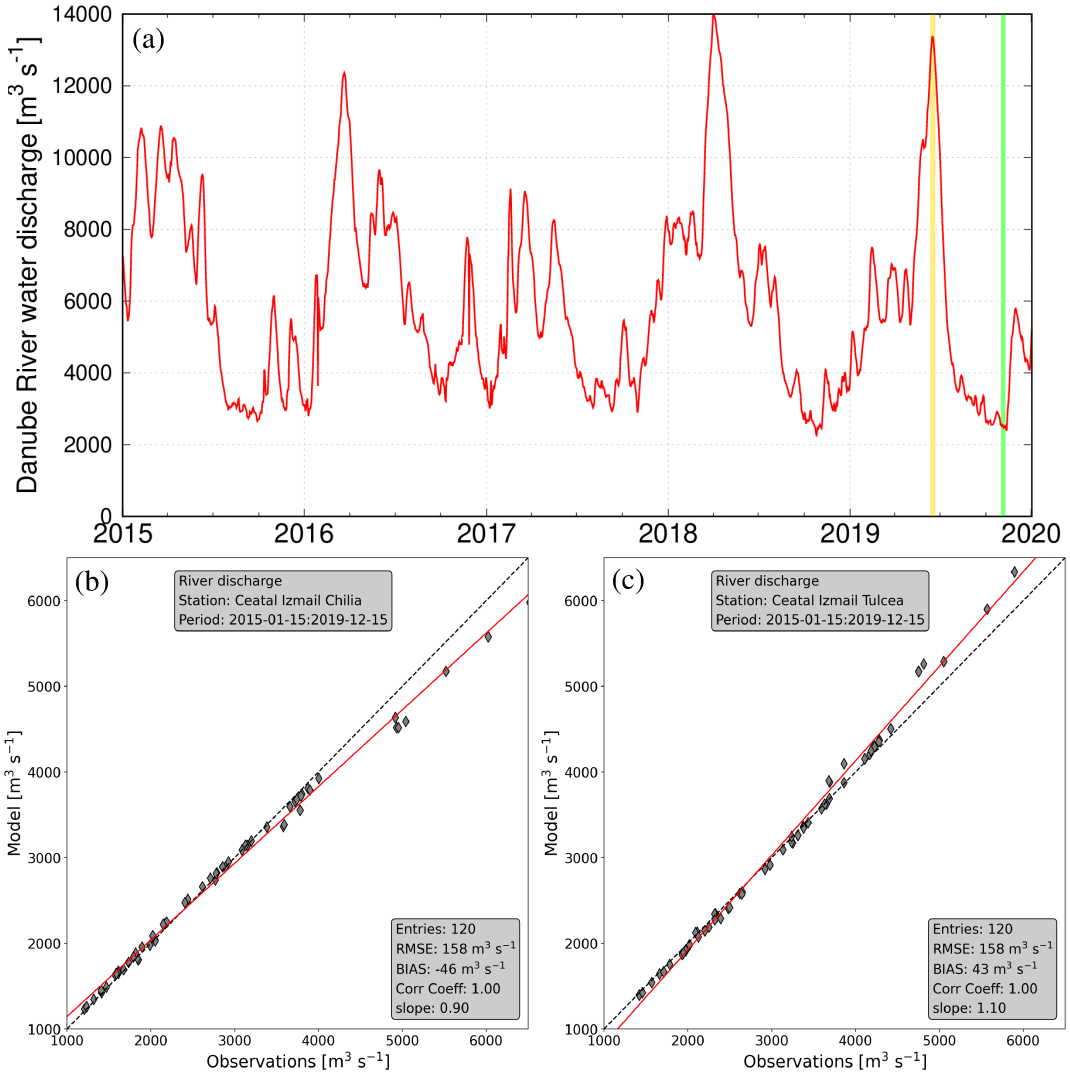


**Figure 2.** Danube River water discharge timeseries (a) and scatter plots of observed and modelled river discharge in the Chilia (b) and Tulcea (c) river branches. The gold and green bars in panel (a) indicate the flood and drought conditions considered in Figs. ~~6~~5b and ~~6~~5c. The gray diamonds and the red lines in panels b and c represent the scatter data and the line of best fit, respectively.

225 (e.g., Constanta in July-August and Mangalia in March). The statistical analysis revealed that RMSE and CC in Constanta and Mangalia are ~~3.4~~6.5 cm and ~~0.64~~0.66, and 7.8 cm and 0.55, respectively (Table 1). It must be noted that the ~~performances~~ performance of the coastal model in reproducing sea levels ~~are directly dependent~~ is strongly determined by the open boundary conditions, therefore any discrepancy ~~at the basin scale in the~~ in the sea level simulated by the Black Sea Physics Reanalysis ~~dataset~~ is propagated to the coast~~and needs to be considered~~.

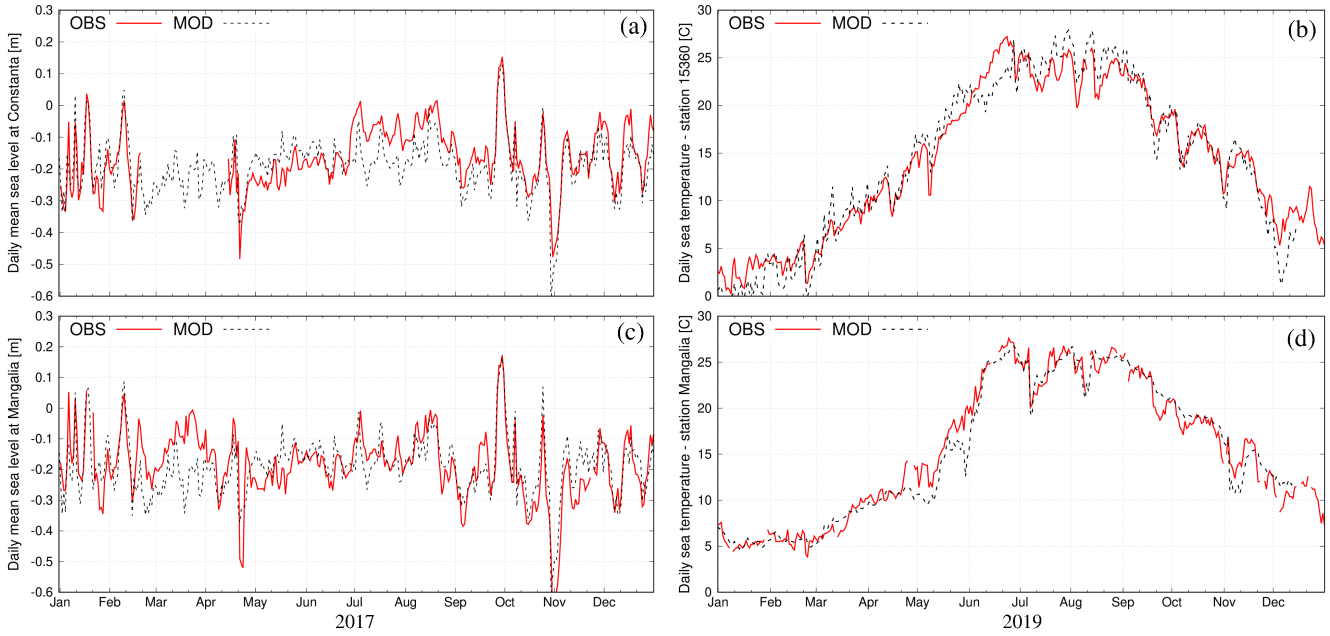


**Figure 3.** Observed (red line) and simulated (black dashed line) sea levels at Constanta (~~top panel~~a) and Mangalia (~~bottom panel~~c)~~for year 2017.~~, and sea temperature at station 15360 (b) and Mangalia (d).

As presented in ~~Figure 4~~ the right panels of Fig. 3 (illustrated for the year 2019 at stations 15360 and Mangalia), the numerical model captures correctly the seasonal variability as well as the short-term fluctuations of the sea temperature in the investigated area. The statistical analysis of the simulated sea temperatures revealed that RMSE is between 1.5 and 1.7 °C and the CC is always above 0.97 (Table 1).

~~Observed (red line) and simulated (black dashed line) daily sea temperatures at station 15360 (top panel) and Mangalia (bottom panel) for year 2019.~~

~~Statistical analysis (in terms of centered RMSE, BIAS and R) of simulated sea temperature at the monitoring stations. StationRMSE (C) BIAS (C) CC 15360 1.7 0.2 0.98 Constanta 1.6 -0.4 0.97 Mangalia 1.5 -0.2 0.97~~

Satellite derived data demonstrate that sea surface temperature in RSLS ~~strongly varies over the year~~ varies strongly over the 2015-2019 period with values ranging from 0 °C in winter to ~~almost 30~~ 28 °C in summer. Spatially SST in the lagoons has a ~~moderate variance with difference usually~~ small spatial variability with difference among stations lower than 1.5 °C. To assess the ~~performance of the modelwe extracted~~ model's performance, we extracted water temperature values from the simulation results ~~daily averaged water temperature values~~ in the surface layer at the location and ~~timing of~~ time corresponding to the satellite SST data. The statistical comparison between model results and observations reported in Table 1 (RMSE = 1°C, BIAS = 0.3°C, CC = 0.97, slope = 0.99) demonstrated that SHYFEM can represent well both the spatial and temporal variability revealed by satellite data.

## 3 Results

The modelling results are presented and analyzed separately for the main water compartments forming the delta: the river network (section 3.1), the coastal sea (section 3.2) and the lagoons (section 3.3). The assessment of the impact of the different lagoon-sea reconnection interventions is included in section 3.3.1.

### 3.1 Water division in the river network of the delta

The Danube Delta~~River network is formed~~ 's river network comprises a highly complex system of hundreds of natural and artificial channels, streams, ~~and lakes. The numerical model could not resolve such a high morphological complexity and was designed to represents the more relevant water courses. It can therefore be used to estimate the~~ marshes, and lakes, whose morphological complexity exceeds the resolution capabilities of the current model implementation. The model was configured to represent only the most hydraulically significant watercourses, enabling the estimation of water discharge distribution among the ~~different~~ principal river branches. Here, the water fluxes were extracted for several river sections and averaged over the simulation period (2015-2019) to estimate the relative ~~load~~ runoff (in %) of each branch with respect to the ~~total~~ average Danube River discharge ~~(~~imposed at the open boundary of Isaccea ~~). We point out that the model estimate of the water division into the multiple branches of the delta is very sensitive to the accuracy of the morphological and bathymetric datasets used to create the numerical grid, which - as mentioned in section 2.3 - has been validated only for the upper part of the delta river network. Moreover, the river discharge division among branches can vary in different flow regimes.~~ ($6000\ m^3\ s^{-1}$). The average water division values are reported in Fig. ~~5~~4. Unless otherwise specified, the reported values refer to averages over the whole 2015-2019 simulation period.

The Danube discharge firstly subdivides into the Chilia and Tulcea branches, which have an average fraction of 46.3 and 53.7 %, respectively, this well reproducing the observed distribution. The Chilia branch in the northern part of the delta is characterized by a complex network of secondary arms that depart and rejoin to the main channel. 20 km from the sea, Chilia bifurcates into the Ochakiv (also known as Ochakov) channel (10.6 %), that downstream originates four mouths, and the Stari Stambul Vechi (33.4 %) channel, which splits into Novo Stambul (14.3 %) and Chilia (19.1 %) outflows. The 18 km long Tulcea distributary bifurcates into the Sulina branch, carrying almost 29.7 % of the Danube waters to the sea, and the Sf. Gheorghe (25.7 %) branch flowing through the southern part of the delta. A small fraction of the Sf. Gheorghe discharge is captured by the Dunavăţ (0.6 %) and Dranov (0.4 %) canals that flow down into the Razelm Lagoon. Just before flowing into the Black Sea, the Sf. Gheorghe branch separates in the Olinca-Turceasca channel (0.4 %), flowing into the Sahalin Lagoon (0.4 %), and the main mouth (24.3~~%)~~ %).

We point out that the model estimate of the water division into the multiple branches of the delta is very sensitive to the accuracy of the morphological and bathymetric datasets used to create the numerical grid, which - due to lack of observations as mentioned in section 2.3 - has been validated only for the upper part of the delta river network. However, the simulated distribution of the Danube's mean discharge between the Chilia, Sulina and Sf. Gheorghe (46.3 %, 29.7 % and 25.7 %, respectively) is similar to the results reported by Nichersu et al. (2025) (45 %, 34 % and 21 %, respectively). It is worth noting

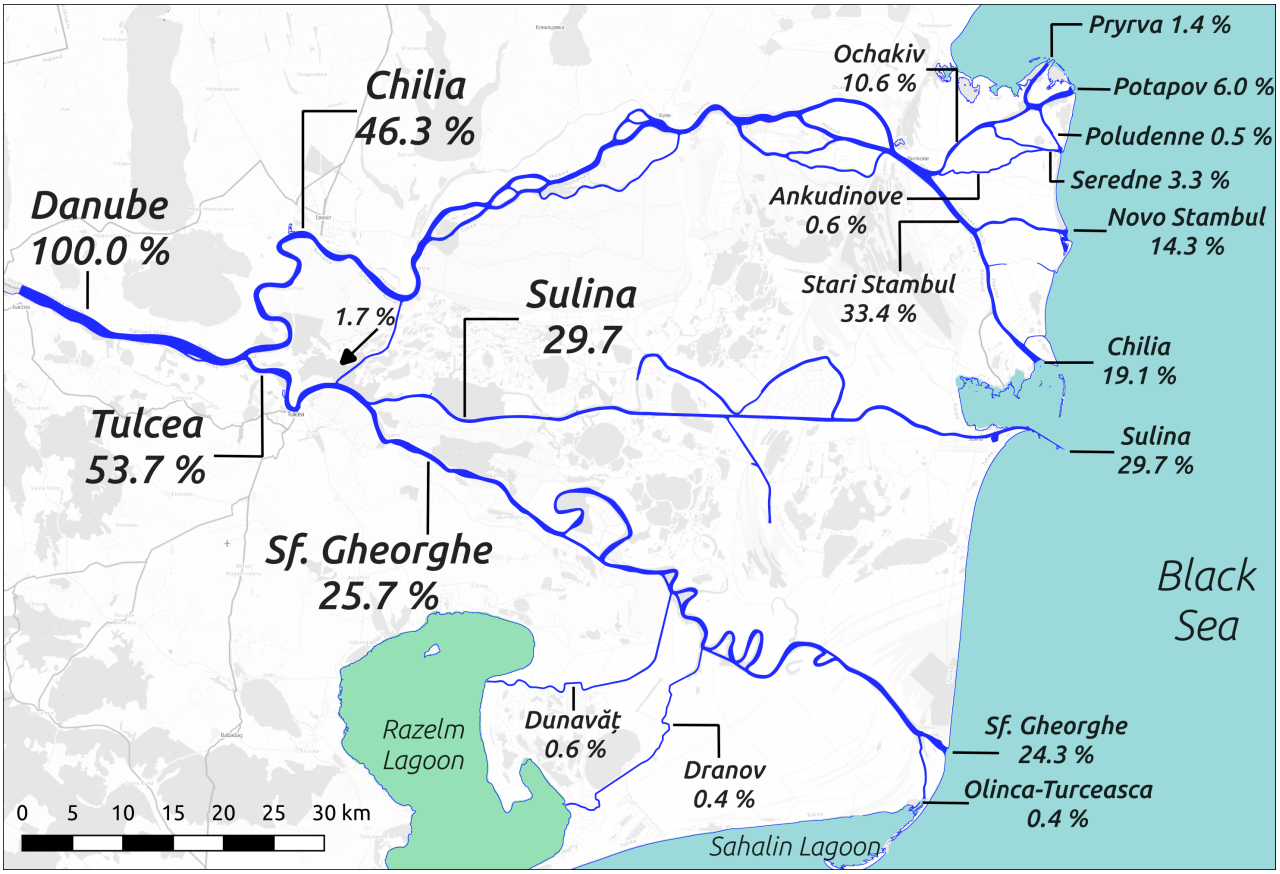


**Figure 4.** Modelled average water diversion within the Lower Danube River downstream of Isaccea. Background: ©OpenStreetMap contributors 2024; distributed under the Open Data Commons Open Database License (ODbL) v1.0.

that the river discharge division among the main branches has been altered by human interventions (Constantinescu et al., 2023; Bloesch et a
280 .

### 3.2 Spatial and temporal variability of coastal dynamics

The dynamics in coastal areas at the river-sea interface is generally determined by the mixing processes induced by the interaction of ~~the river plume~~ river outflow and coastal currents, mainly driven by the open sea circulation and wind ~~(Garvine, 1995; Fong and Geye~~ ~~. Similarly, in~~ (Garvine, 1995; Fong and Geyer, 2002; Bellafiore et al., 2019). Along the coast, these processes create peculiar
285 hydrodynamic patterns, the so-called river plumes, having thermohaline characteristics and buoyancy that allow to distinguish them from seawater. The river plume extension delineate the coastal Region Of Freshwater Influence (ROFI; Simpson et al., 1993) .

In front of the Danube Delta, the general coastal circulation (determined averaging the values over the whole simulated period) reflects these processes with the several branches of the multiple-mouth delta forming separated freshwater plumes having shape and dimension defined by amount of water carried out by the different river branches and the coastline characteristics (Fig. 6~~5~~a). ~~The region of freshwater influence (ROFI; Simpson et al., 1993) extends on average~~Indeed, the largest plume is found south of the Sulina mouth, where the 8 km long artificial jetty enhances the offshore spread of riverine waters and creates a well-defined recirculation structure. It has to be noted that this plume is reinforced by the freshwater discharged by the nearby Chilia mouth. Well-defined plumes can be also recognized out of the Sf. Gheorghe, Novo Stambul and Potapov mouths. On average, the ROFI associated with the Danube River extends for about 15 km offshore the river mouths. As illustrated in Fig. 5d, the freshwater inputs determine a stratified water column along the coast, with Black Sea waters (defined here as having salinity higher than 16 g $L^{-1}$) located on average below 5 to 10 m from the surface. A low-intensity (< ~~10 cm~~ 0.1 m $s^{-1}$) southward current characterize the shelf area which is also influenced by the long-shore dynamics induced by the rivers flowing along the northwestern Black Sea coast ~~(Southern Bug, Dniestr and Dniepr; Bellafiore et al., in review). A well-defined recirculation structure can be identified south of the 5 km long artificial jetty of the Sulina mouth~~(Southern Bug, Dniestr and Dniepr; Miladinova et al., 20
. The lagoon system is on average characterized by very low currents (in the order of a few cm $s^{-1}$) and salinity ranging from 1 to 4 g $L^{-1}$, with the Sinoie Lagoon being saltier than the Razelm lagoon due to the inflow of marine waters through the Edighiol and Periboina inlets.

The hydrodynamics of the whole area is strongly variable in time and space depending on Danube River discharge and other forcing (e.g., wind, heat fluxes, long-shore currents). ~~Indeed, such a variability is illustrated in Figs. 6b and 6c presenting examples of the dynamics (in terms of current velocity and salinity)~~ As examples of a such a high variability, we analysed the dynamics in the investigated area during ~~summer (16~~ two events having different hydro-meteo-marine conditions: 1) a summer event (15 June 2019) ~~calm weather~~ with peak river discharge (~~13000~~ 13,000 $m^3$ $s^{-1}$) and ~~autumn~~ northerly wind (Figs. 5b and Figs. 5e), and 2) an autumn event (11 November 2019) ~~windy (northerly)~~ with low river discharge (~~2400~~ 2,400 $m^3$ $s^{-1}$) ~~autumn conditions, respectively.~~

and southerly wind (Figs. 5c and 5f). The high freshwater input during peak Danube River flow extends ROFI far offshore and to the south, determining a reduction in salinity over a large portion of the coastal area and the enhancement of the southward surface coastal currents up to ~~60 cm~~ 0.6 m $s^{-1}$ (Fig. 6~~5~~b). During peak river flow and northerly wind conditions, vertical mixing processes near the coast occupy the whole water column (Fig. 5e). On the contrary, during low river discharge, the surface coastal ~~dynamics~~ dynamic is mainly driven by the wind. The autumn event ~~present~~ presented in Fig. 6~~5~~c is characterized by a general northward surface transport of saline waters with the ROFI limited to river plumes extending north-eastward for a few km from the river mouths. During such an event, the water column in front of the delta is well mixed except for a surficial 2 m thick layer in front of the main river branches (Fig. 5f).

~~A season analysis was performed to compute the standard deviation (hereinafter STD, considered here as a metric of~~

The analysis of the sea temperature results during events of southerly wind revealed the presence of small scale near-shore patterns located between the river mouths and having thermo-haline characteristics different from the surrounding areas (Fig. 6). The vertical alongshore sea temperature transect presented in Figs. 6c and Figs. 6d indicate an upwelling-driven

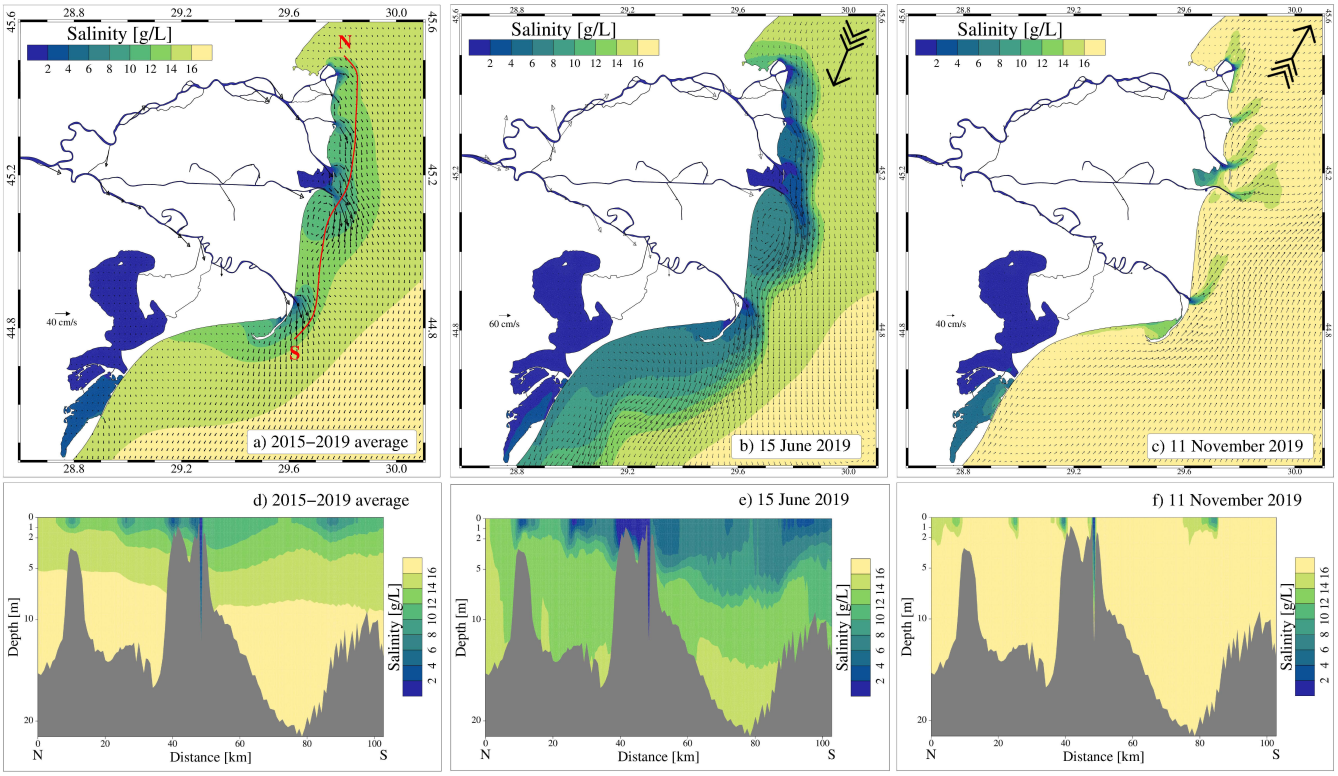


**Figure 5.** Surface salinity and current velocity maps, and N-S salinity transects: a) and d) average values over the 2015-2019 period; b) and e) instant values on 15 June 2019; c) and f) instant values on 11 November 2019. The arrows in the top right corner of panels b and c indicate the wind direction.

transport of marine waters from deeper layers to the coastal zone, enhancing mixing between open sea and riverine waters. The presented analysis indicates that these peculiar features are generated by upwelling processes induced by the action of southerly winds blowing along the coastline and interacting with the river outflow.

To analyse the temporal variability ~~) of the multi-year model results over the whole domain and for each of the~~ of the coastal dynamics, the model results were processed to computed the standard deviation (hereinafter STD) of the month of all years belonging to the four seasons (winter=DJF, spring=MAM, summer=JJA, fall=SON). The surface current variability is higher in winter (Fig. 7a) and spring (Fig. 7b) with STD values above ~~50 cm~~ 0.5 m $s^{-1}$ in a coastal strip extending from the Sulina mouth down to the end of the Sahalin spit. During summer (Fig. 7c) and fall (Fig. 7d) the highest current velocity variability is found south of the Sf. Gheorghe mouth. The highest variability in the surface salinity is found during spring (Fig. 7f) and summer (Fig. 7g) months with STD values above 3 g $L^{-1}$ characterizing large areas in front of each river mouth and a large coastal band south of the delta. The freshwater ~~input from the multiple mouths show a similar~~ discharged by the different branches determine a similar coastal salinity pattern in winter (Fig. 7e) and fall (Fig. 7h)~~but with lower STD values~~. These findings ~~are highly correlated with~~ can be explained by the variability of the Danube River discharge, that usually peaks in spring or early

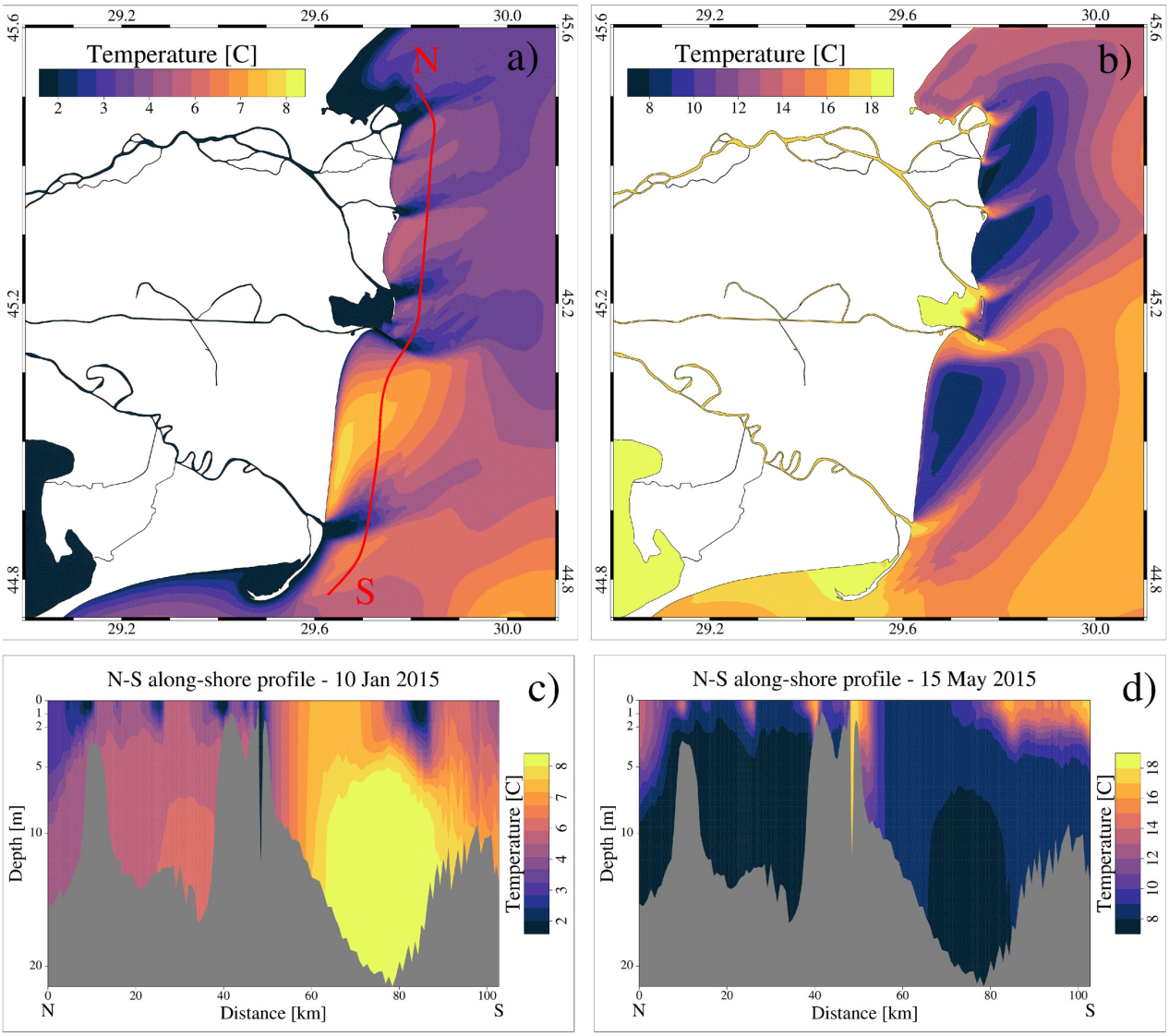


**Figure 6.** Map of sea surface temperature and north-to-south alongshore transect of sea temperature for the 10 January 2015 (a and c) and 15 May 2015 (b and d). The transect location is indicated with a red line in panel a.

summer, while drought conditions are generally found in autumn (Fig. 2a), and the winds (either northerly and southerly), that are generally stronger in winter and autumn (Bajo et al., 2014).

### 3.3 ~~River-lagoon-sea connectivity~~Lagoons' water exchange, mixing and renewal capacity

The Razelm Sinoie Lagoon System is a ~~choked water body receiving Danube freshwater from the Dunavăţand Dranov canals and exchanging waters with the Black Sea via~~ transitional coastal environment connected to the Danube River and the Black

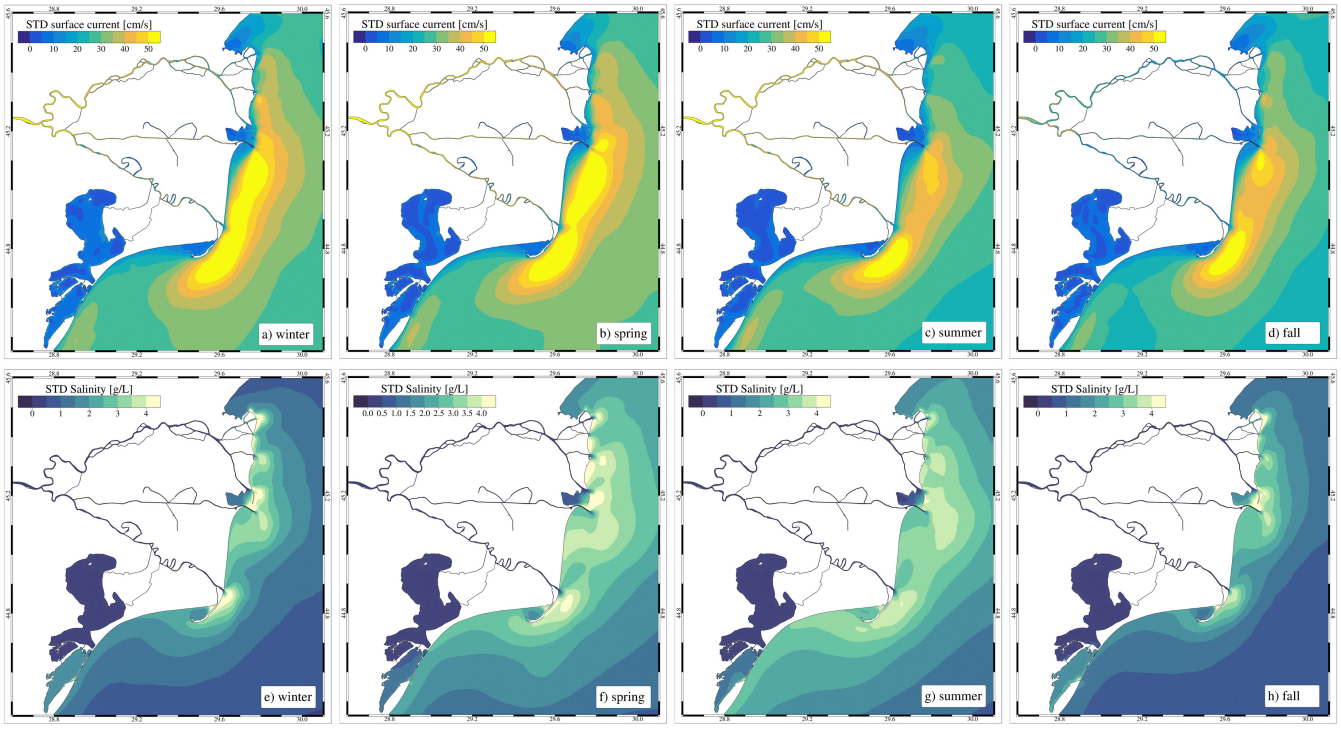


**Figure 7.** Seasonal standard deviation of surface currents (panels a, b, c and d) and surface salinity (panels e, f, g, and h).

Sea. The lagoon's circulation is influenced by the freshwater inflow, the coastal sea level and the wind action over the system. Such dynamics are well illustrated in Figure 8, which presents daily values from 2018 for Danube River discharge, wind speed and direction in the RSLS, sea-lagoon (Sinoie) water level differences, and total water and salt fluxes through the Edighiol and Periboina inlets~~(Dinu et al., 2015). Here water fluxes and water renewal times are used as metrics for investigating the water exchange, mixing and the time a water particle spend into the lagoon system~~.

The water level in the Sinoie Lagoon is generally higher than in the coastal area particularly during flood river conditions (e.g., from March to May 2018). However, the model results show high temporal variability induced by the wind action over the lagoons and the coastal sea. It must be noted that the water flux is not linearly dependent on the water level gradients confirming that the flow between the lagoon and the sea is limited by the transport capacity of the Edighiol and Periboina inlets (ad example at the beginning of March). A two-layers flow in the Edighiol inlet may occur when the lagoon-sea water level gradient is small (in the order of a few of cm).

The freshwater inflow from the Dunavăţ and Dranov canals creates, on average, a persistent water level gradient from Razelm Lagoon to Sinoie Lagoon and the adjacent coastal sea (black line in Fig. 9). The water level jumps between the two lagoons and between the Sinoie Lagoon and the open sea indicate that the water exchange between the different water bodies is limited by the transport capacity of the narrow and shallow connecting canals (Canal 2, Canal 5, Edighiol and Periboina

inlets). The internal average north-to south sea level gradient found into both lagoons is determined by the dominant winds from north-easterly direction.

The RSLS has ~~a~~ an average water volume of about ~~1300~~ 1,300 millions $m^3$ and ~~receive on average~~ receives 40 and 22 $m^3$ $s^{-1}$ of freshwater from the Dunavăţ and Dranov canals, respectively. This ~~surplus of~~ excess water entering the lagoons is ~~mainly~~ primarily discharged into the Black Sea ~~through~~ via the Edighiol and Periboina inlets, ~~accounting for a net outflow of 42~~ resulting in a average seaward flow of 58 $m^3$ $s^{-1}$. The average inflow of marine water into the RSLS amounts to 16 $m^3$ $s^{-1}$. Evaporation over the lagoon system overpasses precipitation resulting in a net loss of 20 $m^3$ $s^{-1}$. ~~Moreover, when the Black Sea level is higher than the lagoon water level an inflow of marine waters entering RSLS occurs, estimated to be 16 $m^3$ $s^{-1}$ on average (with peak values of 210 $m^3$ $s^{-1}$).~~ The lagoons receive a total water flux of 78 $m^3$ $s^{-1}$ from the sea and the river. ~~Therefore, the~~ The average fluxes are reported in Table 2.

**Table 2.** Average water fluxes (in $m^3$ $s^{-1}$) between the lagoons and the sea via the Edighiol and Periboina inlets and the new inlets (positive values indicate inflow into the lagoons, while negative values indicate outflow from the lagoon to the sea).

| Scenario | Edighiol and Periboina inlets | | | New inlet | | | Total flow | | |
|---|---|---|---|---|---|---|---|---|---|
| | Net | Outflow | Inflow | Net | Outflow | Inflow | Net | Outflow | Inflow |
| REF | -42 | -58 | 16 | - | - | - | -42 | -58 | 16 |
| A | -21 | -43 | 22 | -23 | -49 | 26 | -44 | -92 | 48 |
| B | -20 | -42 | 22 | -23 | -51 | 28 | -43 | -93 | 50 |
| C | -24 | -45 | 21 | -19 | -28 | 9 | -43 | -73 | 30 |

The basin-wide water ~~flushing time(WFT), defined as the theoretical time necessary to replace the complete volume of the water body with new water and assuming a hypothetical fully mixed basin (Umgiesser et al., 2014), corresponds to~~ flushing time, computed dividing the volume by the incoming fluxes, is 193 days.

The flushing time estimate was used to determine the duration of the water renewal time simulations. In this work, we performed five one-year-long replicas of WRT starting the simulations at the beginning of each year. The dispersion and dilution of the tracer initially released into the lagoons (see section 2.1) are determined by the inflow of new water and internal mixing processes that in the shallow lagoon system are mainly induced by the wind. The ~~spatio-temporal average~~ average (over the five replicas) basin-wide WRT is 241 days (minimum = ~~194 days in 2015~~181 days in 2018; maximum = 333 days in ~~2018~~2017; standard deviation = 63 days) for the RSLS, thus revealing a mixing efficiency (determined as the ratio between WFT and WRT~~can be interpreted as an index of the mixing behaviour of the basin~~) of 0.8~~corresponding to a well-mixed water system (Umgiesser et al., 2014)~~.

The spatial and temporal variability of river, ocean and meteorological conditions affects the river-lagoon-sea fluxes as well as the internal mixing in the lagoons, and consequently the WRT computation. Indeed, ~~a marked west-to-east~~ the difference in WRT across the different years primarily reflects the freshwater input into the lagoons that mainly drives the river-lagoon-sea fluxes and therefore the flushing of the lagoon waters. Indeed, the minimum (181 days) and maximum (333 days) basin-wide WRT values are found in the flood (2018) and drought (2017) years, respectively (Fig. 2). A secondary, but not negligible, role

is played by the wind which, in 2018 was characterized by frequent and intense Northerlies that enhanced internal mixing and favored the outflow from the lagoon towards the sea. Spatially, a marked east-to-west WRT gradient (from 50 to more than 300 days) is evident in the RSLS, with the Razelm Lagoon having lower values than the Sinoie Lagoon (Fig. ~~8~~10a). This is because the new (fresh) waters enter the Razelm Lagoon from the Dunavăţ and Dranov canals and are subsequently mixed and transported to the Sinoie Lagoon. The input of marine waters through the Edighiol and Periboina inlets has a limited effect on the local WRT, which resulted mostly influenced by the outflow of tracer. Salinity has a limited variability over the RSLS, with values ranging from 1 to ~~5 g~~8 g $L^{-1}$ and where the higher values are found in area of the Sinoie Lagoon near the Edighiol and Periboina inlets (Fig. ~~8b~~10e).

## 3.4 ~~Assessment of lagoon-sea reconnection solutions~~

### 3.3.1 Assessment of the impact of lagoon-sea reconnection solutions

As illustrated in previous section, the RSLS is a large and shallow water body separated from the sea by narrow sandy barriers and with limited renewal capacity. In ~~the past, the lagoons were connected to the sea via several inlets, while nowadays only the Periboina and Edighiol connections are active. Restoring the lagoon-sea water exchange via dredging of a new 1.5 m depth channels is therefore under consideration by local communities and authorities, as part of the activities developed under the framework of the Horizon Europe Project DANUBE4all (). In~~ this study, we use the modelling ~~framework~~ setup for the period 2015-2019 to evaluate the effects of several reconnection solutions (Fig. 1c) on the river-lagoon-sea exchange, water renewal time and salinization.

The numerical model results of the different simulations were processed to estimate the lagoon-sea water exchange through the inlets (the two existing and the newly designed) and the values are reported in Table 2. The ~~hindcast simulation~~ reference run presented in previous sections is ~~here considered the reference run (hereinafter REF) and~~ used as a basis for comparison for the *what-if* scenarios.

~~Average water fluxes (in $m^3$ $s^{-1}$) between the lagoons and the sea via the Edighiol and Periboina inlets and the new inlets (positive values indicate inflow into the lagoons while negative values indicate outflow from the lagoon to the sea). Net Outflow Inflow Net Outflow Inflow Net Outflow Inflow REF -42 -58 16 - - - -42 -58 16 A -21 -43 22 -23 -49 26 -44 -92 48 B -20 -42 22 -23 -51 28 -43 -93 50 C -24 -45 21 -19 -28 9 -43 -73 30~~

Opening a new inlet has a significant effect on the lagoon hydrodynamics altering the water budget of the basin and the fluxes through the existing Edighiol and Periboina inlets, which generally resulted to be enhanced ~~towards~~ inflow into the lagoon and reduced ~~towards the sea~~outflow out of the lagoon (Table 2). The net flow between the lagoons and the sea is not ~~significant~~ significantly altered (about 40 $m^3$ $s^{-1}$), being mostly determined by the river inflow into the lagoon. However, opening a new inlet increases up to four times the total inflow of marine waters into the lagoon with the respect of the reference simulation, with the solutions planned for the Razelm Lagoon (A and B) having a higher effect on the fluxes than the ones designed in the Sinoie Lagoon (C).

Connecting the Razelm Lagoon with the Black Sea with solutions A and B do not only allow the inflow of marine waters but also changes the water level of the two basins (red and blue lines in Fig. 9) decreasing the water exchange between the two lagoons and the outflow via the existing inlets (Table 2). On the contrary, solution C (green line in Fig. 9) affects water levels mostly in the Sinoie Lagoon and the fluxes with the Black Sea but has a limited impact on the Razelm basin.

Because of these changes in the ~~lagoon-sea~~ water level and fluxes, the water renewal capacity and the salinity increase (lower water renewal time values). The average WRTs decrease to 191, 190 and 230 days in scenarios A, B and C, respectively. The spatial distributions of WRT illustrated in Fig. ~~9~~ 10 clearly reflect the changes in the lagoon-sea fluxes. Therefore, solutions A (Fig. ~~9a~~10b) and B (Fig. ~~9b~~10c), are the ones determining a more significant decrease in the water renewal times~~(> 50 days with respect to the REF simulation)~~, especially in the southern part of the Razelm Lagoon and in the Sinoie Lagoon where the WRT values decrease by up to 80 days with respect to the REF simulation. Solution C (Fig. ~~9c~~10d) has a moderate effect on WRTs, which is anyway limited to the southern past of the Sinoie Lagoon.

~~Average WRT (panels a, b, c) and salinity (d, e, f) for the considered open free-flow what-ifscenarios. The red dots in panel e indicate the location of the two control points where the salinity timeseries were extracted (Figure 10).~~

The augmented inflow of marine waters through the existing and the new inlets determines a general increase in salinity in the southern part of the lagoons. The highest salinity changes with respect to the REF simulation (Fig. ~~8b~~10e) are found in scenarios A (Fig. ~~9d~~10f) and B (Fig. ~~9e~~10g) in the Sinoie Lagoon where the average salinity increases to more than 5 g $L^{-1}$. As for the water renewal times, solution C (Fig. ~~9f~~10h) has a limited effect on salinity.

To investigate more into details the opening effects on the salinity, we extracted from the simulation results the timeseries in two control stations in the Razelm and Sinoie lagoons identified with red dots in Fig. 910e (Fig. ~~10~~11). Solutions A and B have very similar effects on salinity which ~~in the southern part of the~~ fluctuates between 2 and 8 g $L^{-1}$, and between 6 and 16 g $L^{-1}$ in the Razelm and Sinoie lagoons, respectively. Lastly, solution C has an almost negligible (< 1 g $L^{-1}$) effect on salinity in both lagoons.

## 4 Discussion

The Danube Delta, ~~as~~ like many other coastal systems at the river-sea interface, is composed ~~by~~ of several interconnected water bodies (river branches, coastal lakes, lagoons, shelf sea) having different physicochemical characteristics and influencing each other (Passalacqua, 2017). Here we interpret how cross-scale hydrodynamics and water mass exchanges between river branches, lagoons, and the coastal sea shape renewal and mixing in the Danube Delta, and we assess how these findings generalize to other river-sea systems. Finally we review the implication of the reconnection solutions on the connectivity between the different water bodies. ~~The exchanges of water among these water bodies are regulated by barotropic and baroclinic processes driven by the forcing acting on the area (upstream river discharge, wind, heat fluxes, open sea conditions) . We focus the discuss on the bidirectional interactions and related driving processes separately for the~~

### 4.1 River-sea modelling characteristics, requirements and limitations

Numerical modelling may play a crucial role in guiding evidence-based efforts to protect and sustainably manage coastal transitional systems, such as estuaries, deltas and lagoons. However, to represent the dynamics inside each water basin, as well as the water exchange among them, the numerical tools need to have specific characteristics:

- the representation of the whole land-ocean area through a numerical domain that extends upstream into the river network and offshore into the open sea. Such an approach has been widely adopted to model processes in several deltas and estuaries. Some model applications are saltwater intrusion and compound floods in the Pearl River Delta (China) (Shen et al., 2018; Zhang and Yu, 2025), hydrodynamics and saltwater intrusion in the Po Delta and adjacent coastal area (Italy) (Maicu et al., 2018; Bellafiore et al., 2021), river plume dynamics in the Columbia River (USA) (Vallaeys et al., 2018), flooding in the Mekong Delta (Vietnam) (Thanh et al., 2020), hydrological connectivity in the Wax Lake Delta (USA) (Feizabadi et al., 2024), tidal intrusion in the Ganges-Brahmaputra-Meghna mega delta (Bangladesh) (Bricheno et al., 2016), among others. Similarly, our cross-scale SHYFEM hydrodynamic model implementation allowed the full representation of the Danube river-sea continuum by comprising the delta river network, the Razelm Sinoie Lagoon System and part of the Western Black Sea shelf area. Moreover, it is crucial, at least for the case of the Danube Delta, to represent also the narrow (about 50 m wide) channels connecting the different water compartments ~~. The implication of the reconnection solutions on the connectivity between the different water bodies is finally discussed.~~ (river to river, river to lagoon, lagoon to lagoon, lagoon to sea).

  ~~Danube River to Black Sea.~~

- an adequate horizontal resolution (at least in the order of a few tens of meters) to correctly reproduce the aforementioned river-sea continuum and the complex morphology that often characterizes deltas and estuaries. Particular attention must be paid to describing narrow channels, secondary river branches, and areas subject to periodic wetting and drying, such as tidal marshes and river floodplains. To meet this constraint and limit computation time, unstructured or flexible mesh models with variable element resolution, such as the SHYFEM model adopted in this study, are preferable to structured mesh models (rectangular grids) (Teng et al., 2017; Umgiesser et al., 2022). The variable model resolution is of fundamental importance for reproducing the complex morphology of the Danube Delta realizing a seamless transition between different spatial scales, from river branches to the coastal sea. As presented in ~~sections 3.1 and 3.2the Danube flows into the Black Sea via several mouths having different dimension and discharge. Clearly, freshwater determines a stratified water column along the coast with a~~ section 3.2, a relatively high horizontal resolution (in the order of a few hundreds of meters) is required in the coastal sea in front of the river mouths to properly capture the plume dynamics. In contrast, most Black Sea regional models (e.g., Lima et al., 2020; Miladinova et al., 2020) have a coarse resolution ($>$ 2 km) and a simplified representation of the river inputs that does not allow the description of the complex coastal circulation ~~pattern, which is generally characterized by a southward long-shore current and recirculation cells located south of the river mouths (Fig. 6~~patterns highlighted in Figs. 5 and 6.

- a ~~). However, the wind plays a crucial role in determining the direction of the coastal circulation and vertical mixing processes~~ three-dimensional baroclinic approach for representing vertical stratification induced by temperature and

salinity gradients. While a vertically integrated barotropic model is generally sufficient for reproducing the circulation along the river course and in shallow coastal environments, a 3D approach must be adopted in coastal environments influenced by freshwater (Horner-Devine et al., 2015). This is certainly the case of the coastal area in front of the Danube Delta, where, as shown in the transects included in Figs. 5 and 6, the freshwater outflow determines a stratified water column. A 3D modelling approach, coupled with a turbulence closure model, is also essential for accurately capturing the mixing of different water masses and the coastal upwelling that occurs during strong wind events (Figs. ~~6b and 6c). A deeper analysis~~ 5 and 6).

- a robust validation of the model results~~revealed complex vertical dynamics in the coastal areas in front of the delta. The sea surface temperature highlighted the presence of small scale near-shore water bulges located between the river mouths and having thermo-haline characteristics different from~~ . Even if Danube Delta is poorly monitored and we had limited (in space and time) observational datasets, the analysis presented in section 2.3 demonstrates that our SHYFEM model application correctly reproduces hydrodynamics in the different water compartments of the Danube Delta. The model validation could be further enhanced with the availability of additional future observations, particularly river discharge and salinity data. In light of these limitations, there is a clear need for an transnational integrated observation system that combines all available monitoring networks managed by academic and research institutions, national and regional environmental protection agencies and local communities. In this context, the pan-European Research Infrastructure DANUBIUS-RI (the International Centre for Advanced Studies on River-Sea Systems, http://www.danubius-ri.eu/) is building integrated infrastructures - made of observational networks, modelling and forecasting systems, and living laboratories - on ten of the major European river-sea systems, one of which is the Danube Delta (De Pascalis et al., 2025) .

## 4.2 Processes driving the exchange between water bodies

The exchanges of water between the ~~surrounding areas (Fig. 11) . Similar patterns were found by Bellafiore et al. (2019)~~ different interconnected water compartments of the delta are regulated by barotropic and baroclinic processes driven by the forcing acting on the area: upstream river discharge, wind stress, heat fluxes, open sea conditions.

The water flow in the river is predominantly governed by advection, and the redistribution of water over the distributaries is mainly determined by the branch geometry and hydraulic roughness. Nevertheless, the distribution of water discharge can vary considerably under different flow regimes (Maicu et al., 2018; Constantinescu et al., 2023). Our simulation results indicate that the standard deviation of the relative discharge among the Danube Delta branches remains below 0.7 %. Such a low temporal variability can be partially attributed to the omission of the delta floodplain system - comprising channels, wetlands, lakes, and marshes - from the computational domain. Floodplains play a critical role in the Danube Delta by providing flood control, water purification, groundwater replenishment, and habitat for diverse species like fish and birds (Frank et al., 2025). The representation of flood dynamics over floodplains (Ciobotaru et al., 2025) in our modelling system would necessitate further technical development (e.g., a more accurate wetting and drying algorithm) and is beyond the scope of this study.

In the coastal area in front of the ~~Po River Delta. The vertical alongshore sea temperature transect presented in Fig. 11c~~ Danube Delta, the presence of multiple freshwater outlets generates multiple buoyant fluxes that interact laterally modulating coastal mixing (Fig. ~~11d) indicate that warmer (colder)marine waters are transported from the deep layers~~ 5). A similar configuration is relevant to many of the world's major river deltas (e.g., the Mississippi and the Nile; Horner-Devine et al., 2015) and coastal settings with multiple river mouths in close proximity (Warrick and Farnsworth, 2017). The interaction between stratified waters belonging to river plumes and the wind force determines complex coastal dynamics. During northerly wind conditions, the freshwater plumes are constrained close to the coast ~~enhancing mixing of open sea and riverine waters. The presented analysis indicate that these peculiar structures are generated by upwelling processes induced by the action of river outflow and southerly winds blowing along the coastline. A clear indication that~~ and advected to the south. Southerly winds that promote coastal upwelling cause the plumes to thin and be advected offshore due to Ekman transport (Fong and Geyer, 2001) . During these events, upwelling - ~~and not~~ rather than horizontal advection - ~~is occurring in these areas is that their surface temperature is different (~~generates small-scale nearshore patterns between the river mouths, characterized by surface temperatures that are either warmer or colder than offshore waters, depending on the season~~) than the offshore waters.~~

~~Map of sea surface temperature and north-to-south alongshore transect of sea temperature for the 10 January 2015 (a and c) and 15 May 2015 (b and d). The transect location is indicated with a red line in panel a.~~

~~Black Sea to Danube River~~ . Similar patterns were found by Bellafiore et al. (2019) in front of the Po River Delta.

In addition to the river influence on the ~~Black Sea~~ coastal dynamics, during drought periods marine waters can intrude ~~along the river branches altering their water~~the lower part of the river course, altering the water's physicochemical properties. Such a phenomenon, known as saltwater intrusion~~(SWI), is well documented in several coastal systems at the river-sea interface, such as delta and estuaries (Shen et al., 2018; **?**; Bellafiore et al., 2021). The near-bottom value of 2 g $L^{-1}$ is chosen as a marker of SWI (Bellafiore et al., 2021). As illustrated in Figure **??** presenting the maximum bottom salinity over the simulated period, in the Danube Delta~~ , is driven by a three-dimensional estuarine dynamics that determines freshwater flowing on the surface layers and the salt wedge intruding along the riverbed (Valle-Levinson, 2010). According to the reference simulation results, marine waters enter up to 20 km upstream from the mouth in the Chilia ~~(mostly from the Chilia secondary delta branches)~~ and Sulina branches, and up to 7 km upstream from the Sf. Gheorghe mouth. ~~Saltwater intrusion is determined by an estuarine type of dynamic in the lower part of the branches with freshwater flowing on the surface layers and the salt wedge intruding along the riverbed. It is important to point out that saltwater intrusion is one of the major threats in coastal area affecting~~ While saltwater intrusion poses a serious threat to several coastal areas compromising freshwater supplies for agriculture and human use ~~, and ecology in coastal wetlands~~(Li et al., 2025), it has not yet been reported as a major issue in the Danube Delta. The situation is predicted to worsen in the near future due to sea level rise (van de Wal et al., 2024) and decreasing summer runoff ~~(Probst and Mauser, 2023)~~(Probst and Mauser, 2023; Stolz et al., 2025).

~~Maximum bottom salinity computed from the model results over the 2015-2019 period.~~

~~Danube River to RSLS to Black Sea.The Razelm-Sinoie Lagoon System is a transitional coastal environment connected to the Danube River and the Black Sea. Due to the input of freshwater from the Dunavăţand Dranov canals, there exists on average over the 2015-2020 period a water level gradient from the Razelm Lagoon (about 30 cm),~~ The water masses of the

~~Sinoie Lagoon (about 26 cm) and the coastal sea (about 23 cm) (green line in Fig. ??)~~Razelm Sinoie lagoons, as many shallow coastal water systems (Umgiesser et al., 2014), are generally vertically well mixed by the action of the wind. Consequently, the long-term net water transport in the RSLS is mainly barotropic and directed from the ~~river~~ Danube River to the Razelm Lagoon ~~, then to the Sinoie Lagoon and finally to the open sea. The water level jumps between the two lagoons and between the Sinoie Lagoon and the open sea indicate that the flow through the narrow and shallow canals (Canal~~ (via the Dunavăţ and Dranov canals), then to the Sinoie Lagoon (via canals 2 ~~, Canal 5, Edighiol and Periboina inlets) connecting the different water bodies resulted to be hydraulically limited. The internal average north-to south sea level gradient found into both lagoons is determined by the dominant north-easterly wind regime.~~

~~Average water level values along a transect crossing the Razelm Sinoie lagoon systems. Background: ©OpenStreetMap contributors 2024; distributed under the Open Data Commons Open Database License (ODbL) v1.0.~~

~~However, the water level gradients are variable in time depending of the freshwater inflow, the coastal sea level and the wind action over the system. Such a dynamic is well illustrated in Figure ?? reporting for the year 2018 the daily values of Danube River discharge, the sea-lagoon (Sinoie)water level difference, and the water and salt fluxes through the Edighiol and Periboina inlets. The water level in the Sinoie Lagoon is generally higher than in the coastal area particularly during flood river conditions (e.g., from March to May 2018). However, the model results show high temporal variability induced by the wind action over the lagoons and the coastal sea . It must be noted that the water flux is not linearly dependent on the water level gradients confirming that the flow through~~ and 5), and finally to the open sea (via the Edighiol and Periboina inlets~~resulted to be hydraulically controlled (ad example at the beginning of March). A two-layers flow in the Edighiol inlet may occur when the lagoon-sea water level gradient is small (in the order of a few of cm).~~

~~Daily values for the year 2018 of Danube River discharge (a), sea-lagoon water level difference (b), sea-lagoon water fluxes (c) and sea-lagoon salt fluxes (d). Positive values of water and salt fluxes indicate inflow into the lagoons while negative values indicate outflow from the lagoon to the sea. systems.~~

~~Black Sea to RSLS.~~). While the water flow from the river to the lagoons is unidirectional, a bidirectional flow characterizes the water exchange between the lagoons and the Black Sea. ~~The inflow of marine waters~~ Marine waters flow into the lagoon ~~occurs in concomitance of positive sea-to-lagoon water levelgradients. Salinity flux peak values~~ when sea level is higher than the lagoon water level. The barotropic flow of marine waters into the lagoons occurs ~~during inflow of marine waters and are mostly found~~ mostly during autumn and winter drought and windy conditions~~(Fig. ??d)~~. As a result, salinization events of the lagoon environments are sporadic and have a general duration of a few days. The salt content entering the Edighiol and Periboina inlets is advected and diluted in the Sinoie Lagoon and sporadically reaches the Razelm basin (Fig. 8a). The barotropic water exchanges with the river and the sea regulate the renewal capacity of the lagoons, while wind stress modulates internal mixing. Due to the limited degree of water exchange, the Razelm-Sinoie lagoons can be classified as a choked water body, according to Kjerfve (1986). Wind stress actively promotes water circulation within the lagoons, making the RSLS a well-mixed water body, according to Umgiesser et al. (2014).

### 4.3 Anthropogenic influence on river-sea systems

The Danube Delta, as many other coastal transitional systems (Maselli and Trincardi, 2013), has been heavily affected by human interventions (Nichersu et al., 2025, and references therein). Among river-sea systems, lagoons are highly productive areas that support numerous industrial, commercial, and recreational activities (Pérez-Ruzafa et al., 2019). Similarly, the RSLS is subject to economic interests related to fisheries, agriculture, and water-based tourism.

Numerical models have been widely used to evaluate the impact of anthropogenic interventions on coastal environments throughout the simulation of ~~*Implications of the lagoon-sea reconnection solutions.The results presented in section 3.3.1 indicate that a local change in the morphology of the coastal lagoons may alter the general hydrodynamics of the whole system. The Razelm and Sinoie lagoonsare interconnected via two narrow and shallow channels and in the present state the net flow of water is from the Razelm basin, which receives Danube River waters, to the Sinoie basin, which is linked to the Black Sea. Connecting the Razelm Lagoon with the Black Sea with solutions A and B do not only allow the inflow of marine waters but also changes the water level of the two basins (lines red and magenta in Fig.* **??***) decreasing the*~~ *what-if* scenarios (Ferrarin et al., 2013; Umgiesser, 2020; Hariharan et al., 2023; Kolb et al., 2022, among others). In the RSLS, efforts to enhance ecological status and improve water circulation have prompted exploration into the potential impacts of creating a new inlet to strengthen the lagoon's connection with the sea. The findings discussed in section 3.3.1 suggest that even a localized morphological modification can significantly influence the overall hydrodynamics of the lagoon system. Introducing a new inlet leads to a reduction in water ~~exchange between the two lagoons and the outflow via the existing inlets (Table 2). At the same time, the lower water level inside the lagoons favours the barotropic inflow of marine waters resulting in higher salinity and lower water renewal times in both basins (Figs. 9 and 10). On the contrary, solution C (blue line in Fig.~~ **~~??~~**~~) affect water levelsin the Sinoie Lagoon and the fluxes with the Black Sea but have a limited impact on the Razelm basin~~renewal time, which helps mitigate stagnation and enhances ecological conditions. However, it also results in elevated salinity levels. While fisheries and tourist activities would benefit from this intervention, the increased salinization of the lagoon's waters poses a considerable risk to agricultural freshwater resources. To help local authorities and communities manage these issues, the model will next be used to explore several alternative lagoon-sea reconnection solutions.

## 5 Conclusions

This work presents the first cross-scale hydrodynamic model implementation ~~over the whole Danube Delta for representing~~ covering the entire Danube Delta to investigate the river-sea continuum. To ~~address land-sea, river-lagoon-sea and coastal-offshore interactions, the SHYFEM numerical~~ study the hydrodynamic processes driving water exchange and connectivity among the various interconnected water compartments of the delta, the 3D unstructured hydrodynamic SHYFEM model was applied to a domain ~~comprising the lower~~ representing the river network, ~~the coastal lagoons~~coastal lagoons, and part of the shelf sea. A multi-year (2015-2019) hindcast simulation was performed ~~by adopting observed Danube River discharge and reanalysis data for the meteorological fields and the Black Sea boundary conditions as forcing.~~

~~The model validation showed that the processes controlling hydrodynamics and the fluxes among the different water compartments of the Danube Delta were correctly taken into account and represented.~~ using observational data and reanalysis fields as forcings. The developed model was validated by comparing various parameters with the available observations.

The simulation results ~~allowed to quantify the~~ enabled the quantification of riverine discharge distribution among the major branches (Chilia~~, Sulina~~ : 46.3 %, Sulina: 29.7 %, and Sf. Gheorghe~~) and~~ : 25.7 %) and the distributaries of the ~~lower~~ delta river network, ~~thus~~ thereby characterizing the relative ~~relevance~~ significance of the nine river mouths. ~~At the same time, the~~ Such a detailed description of the freshwater ~~discharge~~ outflow into the Black Sea ~~permitted to investigate the~~ enabled the investigation of spatial and temporal variability ~~of~~ in the main oceanographic ~~parameters and identify main processes and drivers. The model results clearly show that such a detailed representation of the river-sea continuum of the multi-mouth delta is fundamental for correctly describing the~~ processes occurring offshore of the Danube Delta. River inputs create a stratified water column along the coast, with Black Sea waters typically found at depths greater than 5 to 10 meters below the surface. The region of freshwater influence ~~, which resulted to be~~ is shaped by the ~~several river inputs and along-shore winds. Moreover, we investigated the hydrodynamics of~~ multiple buoyant fluxes forming coalescing river plumes, and alongshore winds. The predominant northerly wind regime sustains a southward coastal current that enhances the southward propagation of the freshriver plumes. Southerly wind conditions favour coastal upwelling, which enhances the offshore propagation of river plumes and creates entrapped marine water regions between them.

On average, approximately 2,000 million $m^3$ of water per year flows from the Danube River into the Razelm Lagoon via the Dunavăţ Dranov canals. This input of freshwater creates a north-to-south water level gradient in the Razelm Sinoie Lagoon System, ~~looking in particular at the processes determining their flushing and renewal capacity. The average water renewal time of this choked coastal environment connected to both~~ which determines a barotropic flow from the Razelm Lagoon to the Sinoie Lagoon and ultimately to the Black Sea. The inflow of marine waters into the Sinoie Lagoon occurs sporadically during southerly wind events that induce a positive sea-to-lagoon water level gradient. Water exchanges with the Danube River and the Black Sea ~~is estimated in~~ determine the flushing capacity of the RSLS, while wind is the primary driver of horizontal and vertical mixing of the lagoon waters. These processes are accounted for in the simulation of a passive Eulerian tracer, which allowed the estimation of the water renewal time in this interconnected coastal environment. The average water renewal time of the RSLS is 241 ~~± 63 days~~days, with marked interannual variability mainly driven by freshwater input into the lagoons and the wind conditions.

Lastly, the numerical model was used to assess the potential impacts of opening a new inlet (with three different configurations) designed to improve the river-sea-lagoon connectivity. Opening a third connection to the Black Sea would enhance the water exchange between the RSLS and the sea, thereby increasing water flushing and reducing the water renewal time to as slow as 190 days (solutions B). At the same time, the augmented inflow of marine waters significantly increased salinity in the southern and central parts of the RSLS (up to 5 g $L^{-1}$). We demonstrated that this modelling system is a powerful tool ~~that can efficiently be used to evaluate the potential impacts~~ for efficiently evaluating the effects of human interventions in the coastal environment. ~~In this study we considered four lagoon-sea reconnection measures designed for improving the renewal capacity~~

~~of the two lagoons. The model will be next used to explore several other river-lagoon-sea reconnection solutions to help local authorities and communities managing connectivity and salinization in the lagoon environment~~

The applied numerical model and implementation approach are easily exportable to other river-sea environments and can be further developed to support decision-making. An operational version of the Danube Delta model ~~will be also developed for providing forecasts to support decision-making and improving~~ is currently under implementation to provide forecasts that enhance awareness and preparedness ~~to~~ for weather-related risks. The simulated *what-if* scenarios and ~~the~~ forecasting system will ~~constitute~~ form the core of the first digital twin of the Danube Delta.

*Code and data availability.* The community SHYFEM hydrodynamic model is open source (GNU General Public License as published by the Free Software Foundation) and freely available through GitHub at https://github.com/georgu/shyfemcm-ismar.

This study has been conducted using the following public available datasets: the Black Sea Physics Reanalysis (https://doi.org/10.25423/CMCC/BLKSEA_MULTIYEAR_PHY_007_004); the Copernicus European Regional ReAnalysis (https://doi.org/10.24381/cds.622a565a); the 2022 European Marine Observation and Data Network bathymetry (https://doi.org/10.12770/ff3aff8a-cff1-44a3-a2c8-1910bf109f85); in situ sea level and sea temperature data (https://marineinsitu.eu/dashboard/); the Danube River temperature data generated by the Black Sea Catchment model developed by Deltares in the EU project DOORS (https://doi.org/10.5281/zenodo.15675190); The following datasets are not public available and can be requested to the mentioned authorities: the National Institute of Hydrology and Water Management of Romania for the Danube River discharge data; the University of Stirling (UK) for satellite sea surface temperature data; GeoEcoMar (RO) for the 2024 Razelm Sinoie Lagoons, the 2019 Sulina branch and the 2016-2017 Sf. Gheorghe branch bathymetric datasets.

*Author contributions.* CF conceived the idea of the study with the support of AS. ID and CF collected the bathymetric and validation data sets. AS designed the reconnection solution to improve river-lagoon-sea hydrological connectivity. CF and APH performed the numerical simulations and analysed the results. All authors discussed, reviewed and edited the manuscript.

*Competing interests.* The authors declare that they have no conflict of interest.

*Acknowledgements.* The authors wish to thank the National Institute of Hydrology and Water Management of Romania for providing river discharge data at Ceatal Izmail; the European Union's Horizon 2020 DOORS project, grant agreement number 101000518, in particular Jos Van Gils, Hélène Boisgontier and Sibren Loos (Deltares, NL) for providing Danube River temperature data (https://doi.org/10.5281/zenodo.15675190); Nagendra Jaiganesh Sankara Narayanan, Andrew Tyler and Evangelos Spyrakos from the University of Stirling (UK) for providing satellite sea surface temperature data; the Lower Danube River Administration for providing 2023 bathymetric data for Chilia Branch. The bathymetry of the Razelm Sinoie was updated during 2024 activities in the Romanian UESFISCDI "DANUBE4all Support" project (77PHE/ 2024). This study was conducted as part of the DANUBE4all (Restoration of the Danube River Basin for ecosystems and people from mountains to coast; ID 101093985; https://www.danube4allproject.eu/) and iNNO_SED (iNNOvative SEDiment management

in the Danube River Basin; ID 101157360; https://innosed.eu/) projects funded by the European Union under EU Mission “Restore our Ocean and Waters”. This work is part of the activities of the scientific community that is building the pan-European Research Infrastructure DANUBIUS-RI - The International Centre for Advanced Studies on River-Sea Systems (http://www.danubius-ri.eu/).

## References


Androsov, A., Fofonova, V., Kuznetsov, I., Danilov, S., Rakowsky, N., Harig, S., Brix, H., and Wiltshire, K. H.: FESOM-C v.2: coastal dynamics on hybrid unstructured meshes, Geosci. Model Dev., 12, 1009–1028, https://doi.org/10.5194/gmd-12-1009-2019, 2019.

Bajo, M., Ferrarin, C., Dinu, I., Stanica, A., and Umgiesser, G.: The circulation near the Romanian coast and the Danube Delta modelled with finite elements, Cont. Shelf Res., 78, 62–74, https://doi.org/10.1016/j.csr.2014.02.006, 2014.

Barsi, J., Barker, J., and Schott, J.: An atmospheric correction parameter calculator for a single thermal band earth-sensing instrument IGARSS 2003, in: Proceedings of the 2003 IEEE International Geoscience and Remote Sensing Symposium (IEEE Cat. No. 03CH37477), vol. 5, pp. 3014–3016, 2003.

Bellafiore, D., Mc Kiver, W., Ferrarin, C., and Umgiesser, G.: The importance of modeling nonhydrostatic processes for dense water reproduction in the southern Adriatic Sea, Ocean Model., 125, 22–28, https://doi.org/10.1016/j.ocemod.2018.03.001, 2018.

Bellafiore, D., Ferrarin, C., Braga, F., Zaggia, L., Maicu, F., Lorenzetti, G., Manfè, G., Brando, V., and De Pascalis, F.: Coastal mixing in multiple-mouth deltas: a case study in the Po Delta, Italy, Estuarine Coastal Shelf Sci., 226, 106254, https://doi.org/10.1016/j.ecss.2019.106254, 2019.

Bellafiore, D., Ferrarin, C., Maicu, F., Manfé, G., Lorenzetti, G., Umgiesser, G., Zaggia, L., and Valle-Levinson, A.: Saltwater intrusion in a Mediterranean delta under a changing climate, J. Geophys. Res. Oceans, 126, e2020JC016437, https://doi.org/10.1029/2020JC016437, 2021.

~~Bellafiore, D., Shamsnia, S. H., Ferrarin~~

Bloesch, J., Lenhardt, M., and Ionescu, C.~~, Bajo, M., Fach~~: Chapter 8 - Hydromorphological alterations and overexploitation of aquatic resources, in: The Danube River and The Western Black Sea Coast, edited by Bloesch, J., Cyffka, B., ~~Sadighrad, E., Arkin, S. S~~Hein, T., Sandu, C., and Sommerwerk, N., ~~Van Gils~~Ecohydrology from Catchment to Coast, ~~J.~~ pp. 147–164, Elsevier, https://doi.org/10.1016/B978-0-443-18686-8.00001-9, ~~Loos, S~~2025.

Bricheno, L. M., Wolf, J., and ~~Boisgontier, H~~Islam, S.: ~~A model chain for the investigation of the river-sea continuum in the Western Black Sea~~Tidal intrusion within a mega delta: An unstructured grid modelling approach, ~~Ocean Model., in review.~~ Estuarine Coastal Shelf Sci., 182, 12–26, https://doi.org/10.1016/j.ecss.2016.09.014, 2016.

Chen, C., Liu, H., and Beardsley, R.: An unstructured grid, finite-volume, three-dimensional, primitive equations ocean model: application to coastal ocean and estuaries, J. Atmos. Ocean. Techno, 20, 159 – 186, https://doi.org/10.1175/1520-0426(2003)020<0159:AUGFVT>2.0.CO;2, 2003.

Ciobotaru, N., Crăciun, A., and C., R.-D.: Flood hazard assessment in the Danube Delta using 2D hydraulic modeling, Scientific Annals of the Danube Delta Institute, 30, 79–90, https://doi.org/10.3897/saddi.30.160526, 2025.

Constantinescu, A. M., Tyler, A. N., Stanica, A., Spyrakos, E., Hunter, P. D., Catianis, I., and Panin, N.: A century of human interventions on sediment flux variations in the Danube-Black Sea transition zone, Front. Mar. Sci., 10, https://doi.org/10.3389/fmars.2023.1068065, 2023.

Cucco, A., Umgiesser, G., Ferrarin, C., Perilli, A., Melaku Canu, D., and Solidoro, C.: Eulerian and lagrangian transport time scales of a tidal active coastal basin, Ecol. Model., 220, 913–922, https://doi.org/10.1016/j.ecolmodel.2009.01.008, 2009.

D-Flow, F.: Delft3D Flexible Mesh Suite, Deltares, Tech. rep., Deltares, https://www.deltares.nl/en/software-and-data/products/delft3d-flexible-mesh-suite, 2023.

Dan, S., Stive, M., Walstra, D.-J. R., and Panin, N.: Wave climate, coastal sediment budget and shoreline changes for the Danube Delta, Mar. Geol., 262, 39–49, https://doi.org/10.1016/j.margeo.2009.03.003, 2009.

De Pascalis, F., Urbinati, E., Aalifar, A., Alcazar, L. A., Arpaia, L., Bajo, M., Barbanti, A., Barbariol, F., Bastianini, M., Bellafiore, D., Bellati, F., Benetazzo, A., Bologna, G., Bonaldo, D., Bongiorni, L., Braga, F., Brando, V. E., Brunetti, F., Caccavale, M., Camatti, E., Campostrini, P., Cantoni, C., Canu, D., Capotondi, L., Cassin, D., Castelli, G., Celussi, M., Correggiari, A., Cozzi, S., Dabalà, C., Davison, S., Fadini, A., Falcieri, F. M., Falcini, F., Ferrarin, C., Foglini, F., Gissi, E., Ghezzo, M., Grande, V., Guarneri, I., Lanzoni, A., Laurent, C., Lorenzetti, G., Madricardo, F., Manfè, G., Mc Kiver, W., Menegon, S., Moschino, V., Nesto, N., Petrizzo, A., Pomaro, A., Ravaioli, M., Remia, A., Riminucci, F., Rosina, A., Rosati, G., Santoleri, R., Scarpa, G., Scroccaro, I., Stanghellini, G., Solidoro, C., and Umgiesser, G.: The DANUBIUS-RI Supersite of Po Delta and North Adriatic Lagoons: a living lab on transitional environments in the Adriatic Sea, Estuarine Coastal Shelf Sci., 324, 109 453, https://doi.org/10.1016/j.ecss.2025.109453, 2025.

Dinu, I., Umgiesser, G., Bajo, M., De Pascalis, F., Stanica, A., Pop, C., Dimitriu, R., Nichersu, I., and Constantinescu, A.: Modelling of the response of the Razelm Sinoie lagoon system to physical forcing, GeoEcoMarina, 21, 5–18, https://doi.org/10.5281/zenodo.45064, 2015.

EMODnet Bathymetry Consortium: EMODnet Digital Bathymetry (DTM 2022), https://doi.org/10.12770/ff3aff8a-cff1-44a3-a2c8-1910bf109f85, 2022.

Feizabadi, S., Li, C., and Hiatt, M.: Response of river delta hydrological connectivity to changes in river discharge and atmospheric frontal passage, Front. Mar. Sci., 11, https://doi.org/10.3389/fmars.2024.1387180, 2024.

Ferrarin, C., Ghezzo, M., Umgiesser, G., Tagliapietra, D., Camatti, E., Zaggia, L., and Sarretta, A.: Assessing hydrological effects of human interventions on coastal systems: numerical applications to the Venice Lagoon, Hydrol. Earth Sys. Sci., 17, 1733–1748, https://doi.org/10.5194/hess-17-1733-2013, 2013.

Ferrarin, C., Bajo, M., Bellafiore, D., Cucco, A., De Pascalis, F., Ghezzo, M., and Umgiesser, G.: Toward homogenization of Mediterranean lagoons and their loss of hydrodiversity, Geophys. Res. Lett., 41, 5935–5941, https://doi.org/10.1002/2014GL060843, 2014.

Ferrarin, C., Bellafiore, D., Sannino, G., Bajo, M., and Umgiesser, G.: Tidal dynamics in the inter-connected Mediterranean, Marmara, Black and Azov seas, Prog. Oceanogr., 161, 102–115, https://doi.org/10.1016/j.pocean.2018.02.006, 2018.

Ferrarin, C., Davolio, S., Bellafiore, D., Ghezzo, M., Maicu, F., Drofa, O., Umgiesser, G., Bajo, M., De Pascalis, F., Malguzzi, P., Zaggia, L., Lorenzetti, G., Manfè, G., and Mc Kiver, W.: Cross-scale operational oceanography in the Adriatic Sea, J. Oper. Oceanogr., 12, 86–103, https://doi.org/10.1080/1755876X.2019.1576275, 2019.

Ferrarin, C., Penna, P., Penna, A., Špada, V., Ricci, F., Bilić, J., Krzelj, M., Ordulj, M., Sikoronja, M., Duračić, I., Iagnemma, L., Bućan, M., Baldrighi, E., Grilli, F., Moro, F., Casabianca, S., Bolognini, L., and Marini, M.: Modelling the quality of bathing waters in the Adriatic Sea, Water, 13, 1525, https://doi.org/10.3390/w13111525, 2021.

Fong, D. A. and Geyer, W. R.: Response of a river plume during an upwelling favorable wind event, J. Geophys. Res. Oceans, 106, 1067–1084, https://doi.org/10.1029/2000JC900134, 2001.

Fong, D. A. and Geyer, W. R.: The ~~Alongshore Transport of Freshwater in a Surface-Trapped River Plume~~alongshore transport of freshwater in a surface-trapped river plume, J. Phys. Oceanogr., 32, 957 – 972, https://doi.org/10.1175/1520-0485(2002)032<0957:TATOFI>2.0.CO;2, 2002.

Frank, G., Funk, A., Becker, I., Schneider, E., and Egger, G.: Chapter 16 - The key role of floodplains in nature conservation: How to improve the current status of biodiversity?, in: The Danube River and The Western Black Sea Coast, edited by Bloesch, J., Cyffka, B., Hein, T., Sandu, C., and Sommerwerk, N., Ecohydrology from Catchment to Coast, pp. 335–364, Elsevier, https://doi.org/10.1016/B978-0-443-18686-8.00008-1, 2025.

Garvine, R. W.: A dynamical system for classifying buoyant coastal discharges, Cont. Shelf Res., 15, 1585–1596, https://doi.org/10.1016/0278-4343(94)00065-U, 1995.

Geuzaine, C. and Remacle, J.-F.: Gmsh: A 3-D finite element mesh generator with built-in pre- and post-processing facilities, Int. J. Numer. Methods Eng., 79, 1309–1331, https://doi.org/10.1002/nme.2579, 2009.

Giosan, L., Donnelly, J. P., Constantinescu, S., Filip, F., Ovejanu, I., Vespremeanu-Stroe, A., Vespremeanu, E., and Duller, G. A.: Young Danube delta documents stable Black Sea level since the middle Holocene: Morphodynamic, paleogeographic, and archaeological implications, Geology, 34, 757–760, https://doi.org/10.1130/G22587.1, 2006.

Hariharan, J., Wright, K., Moodie, A., Tull, N., and Passalacqua, P.: Impacts of human modifications on material transport in deltas, Earth Surf. Dyn., 11, 405–427, https://doi.org/10.5194/esurf-11-405-2023, 2023.

Hersbach, H., Bell, B., Berrisford, P., Hirahara, S., Horànyi, A., Munoz-Sabater, J., Nicolas, J., Peubey, C., Radu, R., Schepers, D., Simmons, A., Soci, C., Abdalla, S., Abellan, X., Balsamo, G., Bechtold, P., Biavati, G., Bidlot, J., Bonavita, M., De Chiara, G., Dahlgren, P., Dee, D., Diamantakis, M., Dragani, R., Flemming, J., Forbes, R., Fuentes, M., Geer, A., Haimberger, L., Healy, S., Hogan, R. J., Hólm, E., Janisková, M., Keeley, S., Laloyaux, P., Lopez, P., Lupu, C., Radnoti, G., de Rosnay, P., Rozum, I., Vamborg, F., Villaume, S., and Thépaut, J.-N.: The ERA5 global reanalysis, Quart. J. Roy. Meteorol. Soc., 146, 1999–2049, https://doi.org/10.1002/qj.3803, 2020.

Horner-Devine, A. R., Hetland, R. D., and MacDonald, D. G.: Mixing and Transport in Coastal River Plumes, Annu. Rev. Fluid Mech., 47, 569–594, https://doi.org/10.1146/annurev-fluid-010313-141408, 2015.

Kjerfve, B.: Comparative oceanography of coastal lagoons, in: Estuarine Variability, edited by D. A. Wolfe, pp. 63–81, Academic Press, New York, USA, https://doi.org/10.1016/B978-0-12-761890-6.50009-5, 1986.

Kolb, P., Zorndt, A., Burchard, H., Gräwe, U., and Kösters, F.: Modelling the impact of anthropogenic measures on saltwater intrusion in the Weser estuary, Ocean Sci., 18, 1725–1739, https://doi.org/10.5194/os-18-1725-2022, 2022.

Li, M., Najjar, R. G., Kaushal, S., Mejia, A., Chant, R. J., Ralston, D. K., Burchard, H., Hadjimichael, A., Lassiter, A., and Wang, X.: The emerging global threat of salt contamination of water supplies in tidal rivers, Environ. Sci. Technol. Lett., 12, 881–892, https://doi.org/10.1021/acs.estlett.5c00505, 2025.

Lima, L., Aydogdu, A., Escudier, R., Masina, S., Ciliberti, S. A., Azevedo, D., Peneva, E. L., Causio, S., Cipollone, A., Clementi, E., Cretì, S., Stefanizzi, L., Lecci, R., Palermo, F., Coppini, G., Pinardi, N., and Palazov, A.: Black Sea Physical Reanalysis (CMEMS BS-Currents) (Version 1)[Data set], https://doi.org/10.25423/CMCC/BLKSEA_MULTIYEAR_PHY_007_004, 2020.

~~Maicuet al.(2018) Maicu~~

Maicu, F., De Pascalis, F., Ferrarin, C., and Umgiesser, G.: Hydrodynamics of the Po River-Delta-Sea system, J. Geophys. Res. Oceans, 123, 6349–6372, https://doi.org/10.1029/2017JC013601, 2018.

Maselli, V. and Trincardi, F.: Man made deltas, Sci. Rep., 3, 1926, https://doi.org/10.1038/srep01926, 2013.

Miladinova, S., Stips, A., Macias Moy, D., and Garcia-Gorriz, E.: Pathways and mixing of the north western river waters in the Black Sea, Estuarine Coastal Shelf Sci., 236, 106 630, https://doi.org/10.1016/j.ecss.2020.106630, 2020.

Newton, A., Mistri, M., Pérez-Ruzafa, A., and Reizopoulou, S.: Editorial: Ecosystem services, biodiversity, and water quality in transitional ecosystems, Frontiers in Ecology and Evolution, 11, https://doi.org/10.3389/fevo.2023.1136750, 2023.

Nichersu, I., Livanov, O., Mierlă, M., Trifanov, C., Simionov, M., Lupu, G., Ibram, O., Burada, A., Despina, C., Covaliov, S., Doroftei, M., Doroşencu, A., Bolboacă, L., Năstase, A., Ene, L., and Balaican, D.: Chapter 6 - The Danube Delta - The link between the Danube River and the Black Sea, in: The Danube River and The Western Black Sea Coast, edited by Bloesch, J., Cyffka, B., Hein, T., Sandu, C., and Sommerwerk, N., Ecohydrology from Catchment to Coast, pp. 107–122, Elsevier, https://doi.org/10.1016/B978-0-443-18686-8.00002-0, 2025.

Panin, N.: Impact of global changes on geo-environmental and coastal zone state of the Black Sea, GeoEcoMarina, 1, 7–23, 1996.

Panin, N.: Danube Delta: Geology, Sedimentology, Evolution, Association des Sédimentologistes Français, 1998.

Panin, N.: Global changes, sea level rise and the Danube Delta: risks and responses, GeoEcoMarina, 4, 19–29, 1999.

Passalacqua, P.: The Delta Connectome: A network-based framework for studying connectivity in river deltas, Geomorphology, 277, 50–62, https://doi.org/10.1016/j.geomorph.2016.04.001, 2017.

Pein, J., Staneva, J., Mayer, B., Palmer, M., and Schrum, C.: A framework for estuarine future sea-level scenarios: Response of the industrialised Elbe estuary to projected mean sea level rise and internal variability, Frontiers in Marine Science, 10, https://doi.org/10.3389/fmars.2023.1102485, 2023.

Pekárová, P., Mèszáros, J., Miklánek, P., Pekár, J., Prohaska, S., and Ilić, A.: Long-term runoff variability analysis of rivers in the Danube basin, Acta Horticulturae et Regiotecturae, 24, 37–44, https://doi.org/10.2478/ahr-2021-0008, 2021.

Pérez-Ruzafa, A., Pérez-Ruzafa, I. M., Newton, A., and Marcos, C.: Chapter 15 - Coastal Lagoons: Environmental Variability, Ecosystem Complexity, and Goods and Services Uniformity, in: Coasts and Estuaries, edited by Wolanski, E., Day, J. W., Elliott, M., and Ramachandran, R., pp. 253–276, Elsevier, https://doi.org/10.1016/B978-0-12-814003-1.00015-0, 2019.

Probst, E. and Mauser, W.: Climate Change Impacts on Water Resources in the Danube River Basin: A Hydrological Modelling Study Using EURO-CORDEX Climate Scenarios, Water, 15, https://doi.org/10.3390/w15010008, 2023.

Schimanke, S., Ridal, M., Le Moigne, P., Berggren, L., Undén, P., Randriamampianina, R., Andrea, U., Bazile, E., Bertelsen, A., Brousseau, P., Dahlgren, P., Edvinsson, L., El Said, A., Glinton, M., Hopsch, S., and Isaksson, L.and Mladek, R. O. E. V. A. W. Z.: CERRA sub-daily regional reanalysis data for Europe on single levels from 1984 to present, https://doi.org/10.24381/cds.622a565a, 2021.

Shen, Y., Jia, H., Li, C., and Tang, J.: Numerical simulation of saltwater intrusion and storm surge effects of reclamation in Pearl River Estuary, China, Applied Ocean Research, 79, 101–112, https://doi.org/10.1016/j.apor.2018.07.013, 2018.

Simpson, J. H., Bos, W., Schirmer, F., Souza, A., Rippeth, T., Jones, S., and Hydes, D.: Periodic stratification in the Rhine ROFI in the North Sea, Oceanologica Acta, 16, 23–32, 1993.

Stolz, R., Mauser, W., and Probst, E.: Chapter 10 - Climate change-specific consequences for the Danube River Basin and the Black Sea Coast, in: The Danube River and The Western Black Sea Coast, edited by Bloesch, J., Cyffka, B., Hein, T., Sandu, C., and Sommerwerk, N., Ecohydrology from Catchment to Coast, pp. 195–222, Elsevier, https://doi.org/10.1016/B978-0-443-18686-8.00012-3, 2025.

Telemac-Mascaret, O.: TELEMAC-3D Theory guide, Tech. rep., http://wiki.opentelemac.org/, 2022.

Teng, J., Jakeman, A., Vaze, J., Croke, B., Dutta, D., and Kim, S.: Flood inundation modelling: A review of methods, recent advances and uncertainty analysis, Environ. Model. Softw., 90, 201–216, https://doi.org/10.1016/j.envsoft.2017.01.006, 2017.

Thanh, V. Q., Roelvink, D., van der Wegen, M., Reyns, J., Kernkamp, H., Van Vinh, G., and Linh, V. T. P.: Flooding in the Mekong Delta: the impact of dyke systems on downstream hydrodynamics, Hydrol. Earth Syst. Sci., 24, 189–212, https://doi.org/10.5194/hess-24-189-2020, 2020.

Umgiesser, G.: The impact of operating the mobile barriers in Venice (MOSE) under climate change, J. Nat. Conserv., 54, 125 783, https://doi.org/10.1016/j.jnc.2019.125783, 2020.

Umgiesser, G., Melaku Canu, D., Cucco, A., and Solidoro, C.: A finite element model for the Venice Lagoon. Development, set up, calibration and validation, J. Mar. Syst., 51, 123–145, https://doi.org/10.1016/j.jmarsys.2004.05.009, 2004.

Umgiesser, G., Ferrarin, C., Cucco, A., De Pascalis, F., Bellafiore, D., Ghezzo, M., and Bajo, M.: Comparative hydrodynamics of 10 Mediterranean lagoons by means of numerical modeling, J. Geophys. Res. Oceans, 119, 2212–2226, https://doi.org/10.1002/2013JC009512, 2014.

Umgiesser, G., Ferrarin, C., Bajo, M., Bellafiore, D., Cucco, A., De Pascalis, ~~Ferrarin~~F., Ghezzo, M., Mc Kiver, W., and Arpaia, L.: Hydrodynamic modelling in marginal and coastal seas - The case of the Adriatic Sea as a permanent laboratory for numerical approach, Ocean Model., 179, ~~and~~ 102123, https://doi.org/10.1016/j.ocemod.2022.102123, 2022.

Vallaeys, V., Kärnä, T., Delandmeter, P., Lambrechts, J., Baptista, A. M., Deleersnijder, E., and Hanert, E.: Discontinuous Galerkin modeling of the Columbia River's coupled estuary-plume dynamics, Ocean Model., 124, 111–124, https://doi.org/10.1016/j.ocemod.2018.02.004, 2018.

Valle-Levinson, A.: Contemporary Issues in Estuarine Physics, Cambridge University Press, 2010.

van de Wal, R. S. W., Melet, A., Bellafiore, D., Vousdoukas, M., Camus, P., Ferrarin, C., Oude Essink, G., Haigh, I. D., Lionello, P., Luijendijk, A., Toimil, A., and Staneva, J.: Sea Level Rise in Europe: Impacts and consequences, State Planet., 3-slre1, 5, https://doi.org/10.5194/sp-3-slre1-5-2024, 2024.

van Gils, J., Loos, S., and Boisgontier, H.: Simulated fluxes of water, heat, nutrients, fine sediment for 13 large rivers to the Black Sea 2011-2020, https://doi.org/10.5281/zenodo.15675190, 2025.

Vespremeanu-Stroe, A., Preoteasa, L., Hanganu, D., Brown, T., Bîrzescu, I., Toms, P., and Timar-Gabor, A.: The impact of the Late Holocene coastal changes on the rise and decay of the ancient city of Histria (Southern Danube delta), Quaternary International, 293, 245–256, https://doi.org/10.1016/j.quaint.2012.11.039, 2013.

Warrick, J. A. and Farnsworth, K. L.: Coastal river plumes: Collisions and coalescence, Prog. Oceanogr., 151, 245–260, https://doi.org/10.1016/j.pocean.2016.11.008, 2017.

Zhang, A. and Yu, X.: Development of a land-river-ocean coupled model for compound floods jointly caused by heavy rainfalls and storm surges in large river delta regions, Hydrol. Earth Syst. Sci., 29, 2505–2520, https://doi.org/10.5194/hess-29-2505-2025, 2025.

Zhang, Y. J., Ye, F., Stanev, E. V., and Grashorn, S.: Seamless cross-scale modeling with SCHISM, Ocean Model., 102, 64–81, https://doi.org/10.1016/j.ocemod.2016.05.002, 2016.

Zhu, J., Cheng, X., Li, L., Wu, H., Gu, J., and Lyu, H.: Dynamic mechanism of an extremely severe saltwater intrusion in the Changjiang estuary in February 2014, Hydrol. Earth Syst. Sci., 24, 5043–5056, https://doi.org/10.5194/hess-24-5043-2020, 2020.

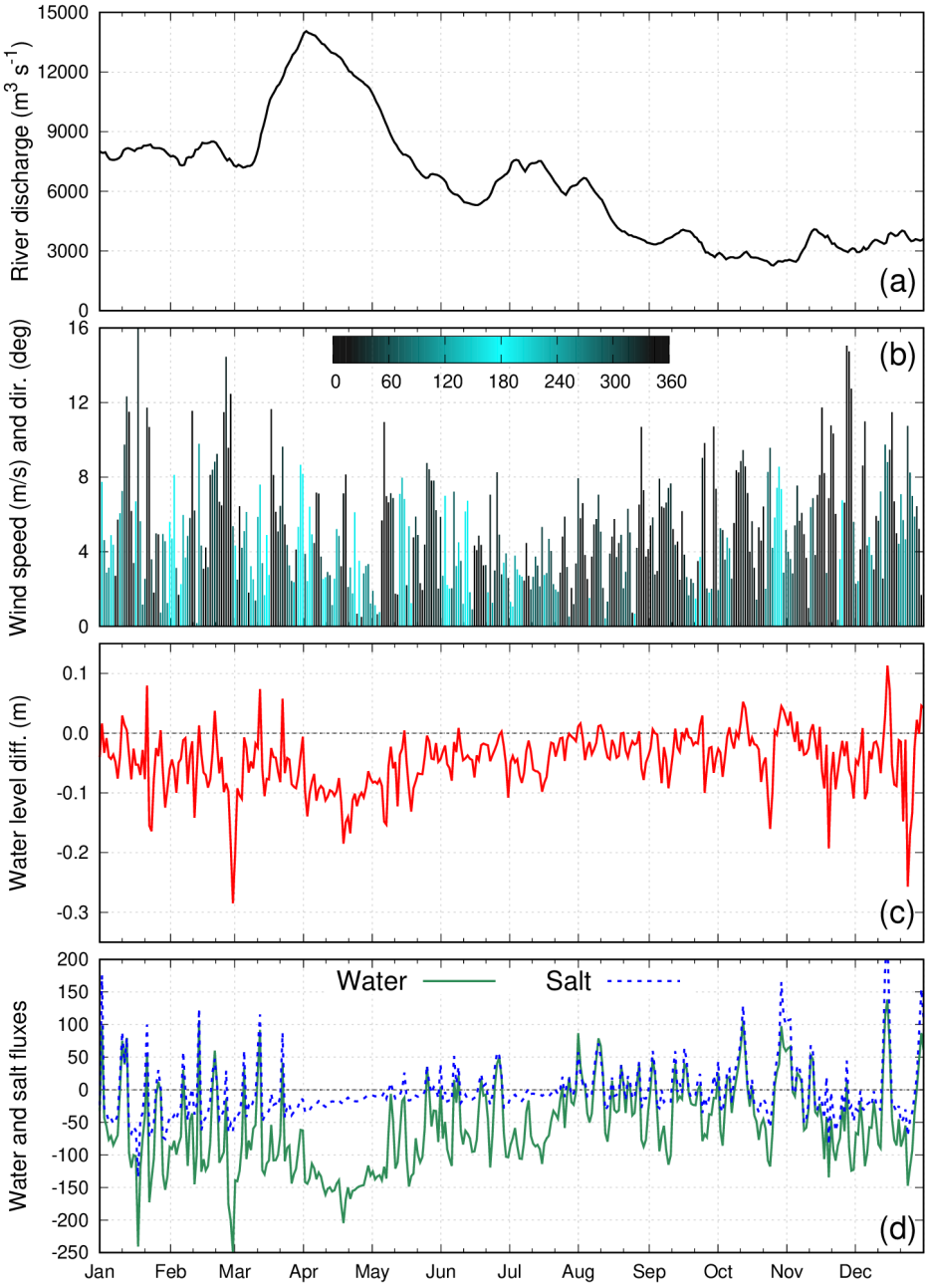


**Figure 8.** (a) Daily values for the year 2018 of Danube River discharge, (b) wind speed and direction (0°means a northerly wind and 180°indicates a southerly wind) in the RSLS, (c) simulated sea-lagoon (Sinoie) water level difference, (d) simulated sea-lagoon water (in $m^3\ s^{-1}$) and salt (in $10^{-1}$ kg $s^{-1}$) fluxes. Positive values of water and salt fluxes indicate inflow into the lagoons, while negative values indicate outflow from the lagoon to the sea. Model results are from the reference simulation.

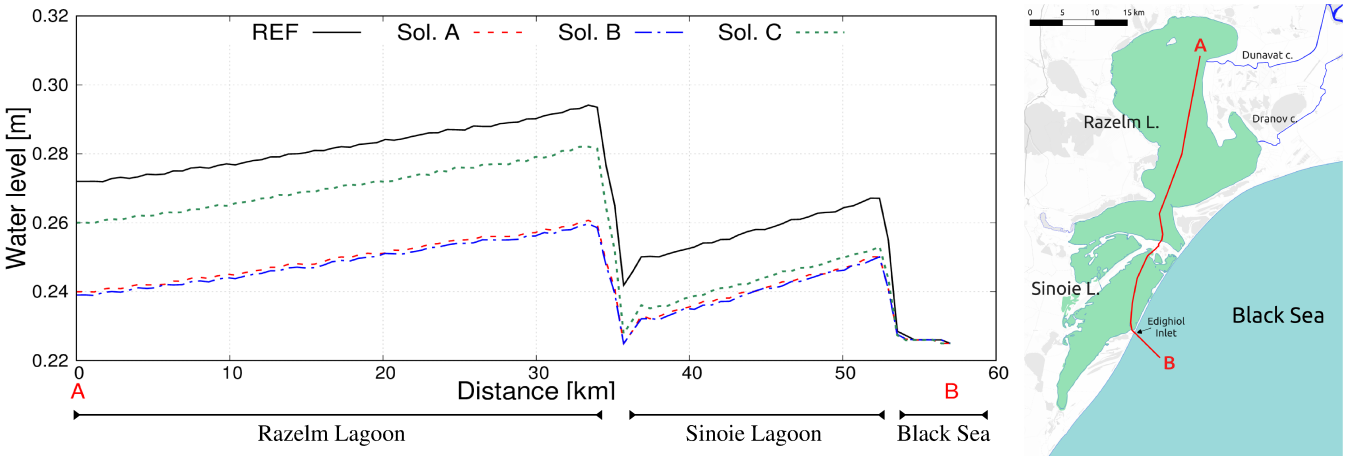


**Figure 9.** Average (over 2015-2019 period) water levels along the AB transect crossing the Razelm Sinoie Lagoon Systems indicated with a red line in the right panel. Background: ©OpenStreetMap contributors 2024; distributed under the Open Data Commons Open Database License (ODbL) v1.0.

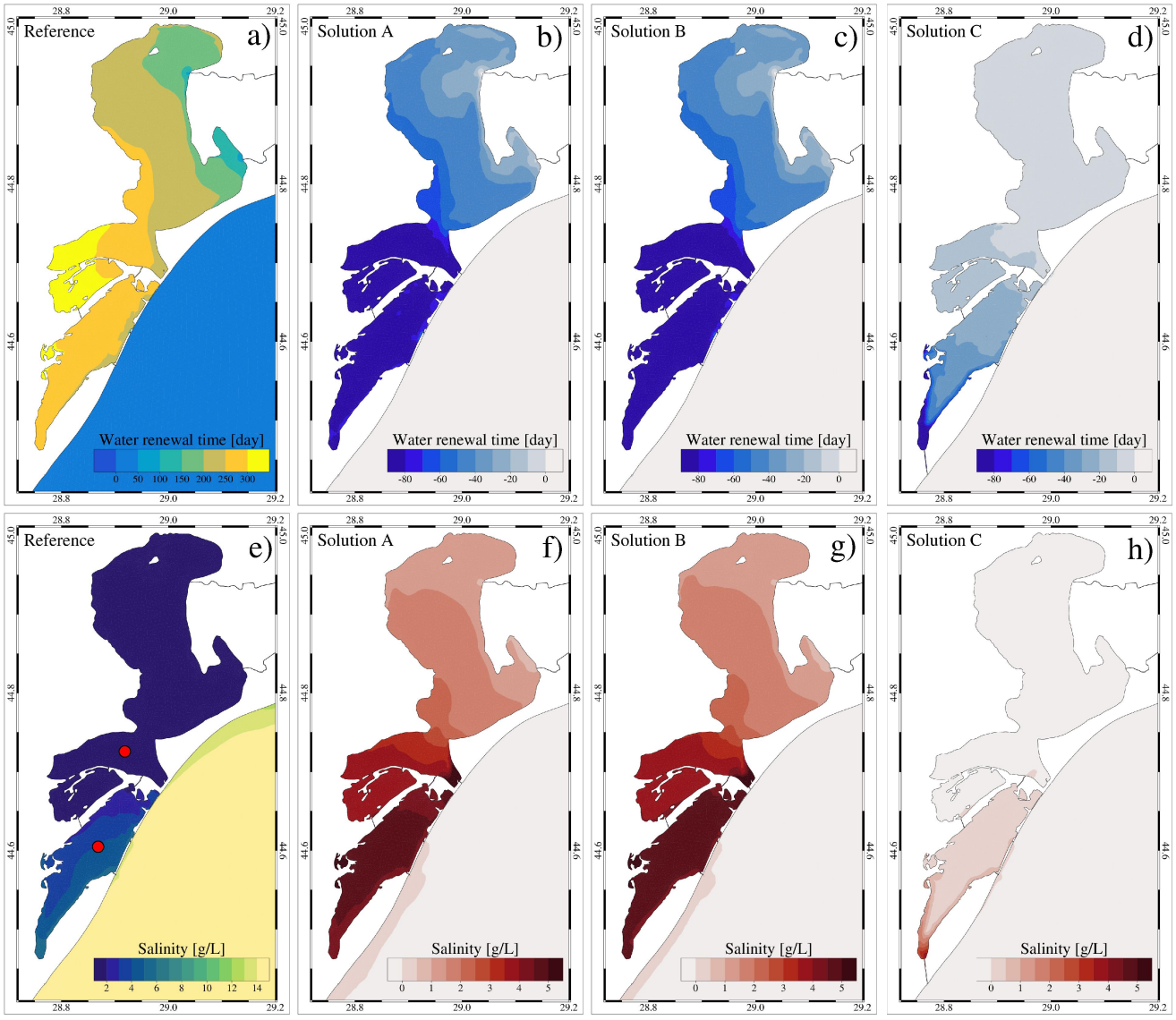


**Figure 10.** Average water renewal time ~~(panel a)~~ and salinity ~~(panel b)~~ over the Razelm Sinoie Lagoon System for the reference simulation (as absolute values) and the reconnection scenarios A, B and C (as difference with respect to the reference run). The red dots in panel *e* indicate the location of the two control points where the salinity timeseries were extracted (Fig. 11).

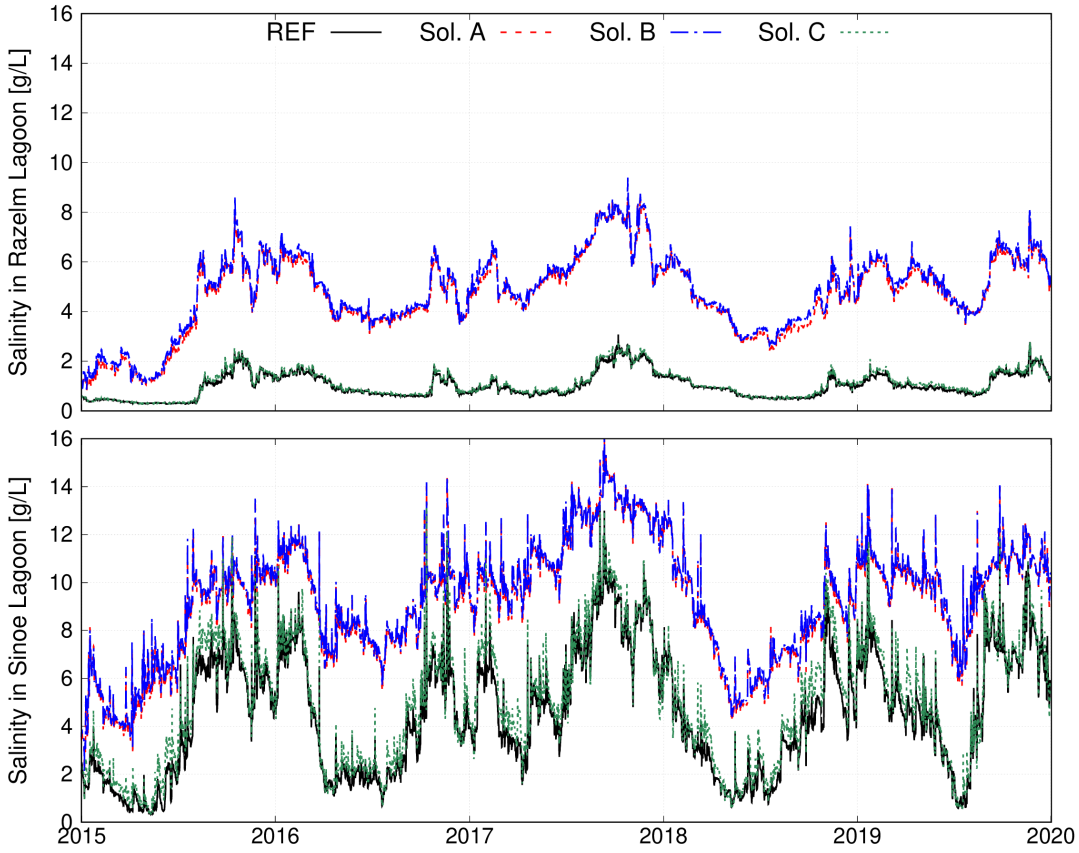


**Figure 11.** Timeseries of modelled salinity extracted in the control points in the Razelm (top panel) and Sinoie (bottom panel).